

Answer to Referee 1

We wish to thank this referee for his/her very insightful comments. In our opinion, addressing these comments has helped us to strengthen the manuscript.

Specific comments

1. *1. First paragraph (line 10-, page 1). The authors summarize the scientific findings that followed the discovery of the Antarctic ozone hole, but they do not cite any study at all (i.e. Chubachi 1984, Molina and Molina 1987, Bowman JAS 1993; JGR 1993, Manney et al. JAS 1994, etc.).*

We added “Solomon (1999; and references therein)”. We also added “Chubachi, S., 1984a and Solomon” (1988; and references therein).

2. *Page 2, line 16. “De la Camara et al (2013) suggested that HTs are representative of cat’s eye structures ...”. McIntyre and Palmer (Nature 1983, JASTP 1984) and Bowman (JAS 1996) might be better references for this suggestion.*

Thanks for pointing this out. We have added McIntyre and Palmer (1983) and Bowman (1996).

3. *Page 2, line 25. “Our goal in the present study is to identify essential features in the filamentation process associated with the breakdown of the polar vortex ...” I think the authors need to explain better the need for this study, putting it more in context. Why is this study interesting? Is this the first time anyone tries to show Lagrangian coherent structures during a sudden warming? What new insights into the dynamics of the polar vortex do you expect to gain from the analysis?*

We have paid close attention to this comment. The Introduction starts with a new paragraph that addresses this concern. We state that the goal is to extract the physical mechanisms underlying notable transport features observed in complex data sets. We gain new insights into the fundamental mechanisms responsible for complex fluid parcel evolution, such as those associated with Rossby wave breaking phenomena, and describe a simple model having the ability to capture transport features, such as filamentation and vortex breaking. We have also added more discussion in the conclusions.

4. *Page 4, line 15. Please cite some works as examples.*

We have added Wiggins (2005) and Samelson and Wiggins (2006).

5. *Page 5, line 26. The authors justify 2-D trajectories on the basis of isentropic motions with timescales of 10 days. If $\tau = 15$ days, that means the trajectories expand $2\tau = 30$ days. Is the 2-D motion approximation still valid? It would be useful to estimate the error growth of the 2-D trajectories (with respect to 3-D trajectories) with increasing τ . Page 5, line 26. The authors justify 2-D trajectories on the basis of isentropic motions with timescales of 10 days. If $\tau = 15$ days, that means the trajectories expand $2\tau = 30$ days. Is the 2-D motion approximation still valid? It would be useful to estimate the error growth of the 2-D trajectories (with respect to 3-D trajectories) with increasing τ .*

We have added a paragraph addressing this comment at the end of section 2.2.

6. *Figure 3, caption. “Notice the change in wind direction from westerly to easterly ... giving rise to the pinching of the SPV”. The change in sign in zonal mean quantities does not reflect a particular change in the horizontal geometry of the vortex. Stratospheric*

warmings have been reported as displacement and split events (roughly wave-1 and wave-2 phenomena), but the zonal mean behavior of the zonal mean wind is rather similar. I would put it the other way round; it is the radical change in the vortex position and/or geometry during stratospheric warmings that gives rise to the change in zonal mean wind direction.

In view of these comments the description of the pinching was rewritten and extended at the end of section 4.

7. Page 9, lines 3-5. *“Finally, the breakup of the SPV on the 24th September 2002 depicted in Fig. 4 b) is caused by the formation of an HT in the interior of the vortex whose manifolds connect the interior and the exterior of the jet, allowing for the interchange of air through the barrier.” From my point of view, the hyperbolic trajectory is a kinematic manifestation of a dynamical process. I am not sure if it is correct to state that the formation of the HT is the cause of the vortex breakdown.*

Throughout the manuscript we have replaced the expression “caused by the formation of a HT” by “occurred when a HT forms”.

8. Page 9, lines 7-8. *Z0 is not independent of Z1 and Z2. In fact, linear theory states that the transient convergence of wave activity decelerates the mean flow, and this in turn affects the propagation and dissipation of the planetary waves.*

The reviewer is correct. In the context of the kinematic model, the modes are given. We have based our specifications of the modes on the observation. The text have been revised to clarify this notion.

9. Page 11, lines 16-18. *In dynamically consistent models, those filaments could be related to wave breaking phenomena, or nonlinear vortex-vortex interactions. What is the reason for their presence in the kinematic model?*

The filaments mentioned by the referee, are related to the presence of hyperbolic trajectories that we link to wave breaking phenomena. In order to illustrate this in more detail we have rewritten section 4. Prior to the figure presenting the filaments mentioned by the referee, the kinematic model is adjusted to a stationary case, in which hyperbolic trajectories can be explicitly calculated as the velocity field is stationary (see new figure 6a)). Then the problem becomes non stationary by imposing a phase speed to the wave 2, and for slowly propagating waves hyperbolic trajectories are identified which are also rotating (see new figure 6b)). The pattern eventually produces filamentation in the pattern of M (see figure 7 a)) by making in the kinematic model the amplitude of wave 2 time dependent.

10. Page 13, lines 12-19 (Figure 7). *I wonder if the amplitude reduction of Ψ_0 and amplification of Ψ_2 used to construct Fig. 7 is somewhat similar to what happened with Z0 and Z2 in the reanalysis data during the split event.*

Yes, we have selected perturbation amplitudes in accordance to the reanalysis data.

11. Section 5. *It is possible that I have not followed the argument here. What are the values of C and h that you need to conserve Q in your kinematic model? Are those values within the range of values used in shallow water models for the study of polar stratospheric dynamics?*

Section 5 has been rewritten and an explicit calculation of the forcing h is reported, that achieves the conservation of potential vorticity Q for one of the proposed Ψ . The

calculation is illustrated for a simple Q choice but it could be repeated for more realistic Q distributions as far as they are defined as piecewise constant functions.

Technical comments:

12. *Figure 1, caption. "... coherent structures above and below the SPV". Please replace above and below with over the South Atlantic and south of Australia.*

Done

13. *Figures 2 and 5 (and some movies). Please improve the color scale, the figures look blurry.*

Contours were added to the figures. Thanks for pointing this out.

Answer to Referee 2

We wish to thank to this referee for his/her very useful comments that have helped us to improve the manuscript and have been addressed as follows:

General comments:

1. *This paper addresses the issue of Lagrangian transport in the Stratospheric Polar Vortex (SPV). The first part of the paper analyzes SPV data from the ECMWF using the technique of Lagrangian Descriptors (LDs, developed over the years by some of the authors of this paper and their collaborators) for a specific time period in September 2002. A three-mode kinematic model which possesses the gross characteristics of the data is then developed, and there is some discussion on how it is possible by adjusting its parameters to mimic certain behaviors of the observational data. The paper is well-written and readable. However, I believe that some more work is needed to show that LDs are relevant to this situation, and that the kinematic model provides useful information. I have expanded on this in my specific comments below. My feeling is therefore that a major revision would be required before being acceptable for publication.*

We have clarified in a new version of the Introduction, the major goals of the article as maybe they were not sufficiently elaborated in original manuscript. The major goal is to gain new insights into the fundamental mechanisms responsible for complex fluid parcel evolution by providing a simple model (a kinematic model). The model allows in a controlled manner to recognize the physical mechanism responsible for the key observed transport features of SPV. In order to highlight the Lagrangian skeleton responsible for transport features both in the stratosphere and in the model, we use a Lagrangian tool, the function M , which has been extensively used in the literature. We consider that the references we provide in Section 2.2 provide a sufficient basis to use this tool, and we do not focus on justifying again in this new paper the efficiency of M in highlighting Lagrangian features, we just use it.

Specific comments:

1. *It seems that the major focus is on modeling the SPV breakdown in September 2002. If trying to use Figure 4 as evidence that LDs provides an excellent way to explain this, then I feel that there must be some comparison to other studies which show this. Beyond a few brief references (page 2, line 27-28), the authors do not seem to do much in this direction. After all, how good are the results of Figure 4? What are the other symptoms of the SPV breakdown what other observations showed that this indeed did break down? (Using Figure 3 is a start but this is using an Eulerian observation to predict something Lagrangian or is it?) And is Figure 4 consistent with any other observations? Several references which might help are: Nishii & Nakamura (Geophys. Res. Lett., 2004), Kruger et al (J. Atmos. Sci., 2005), Taguchi (J. Atmos. Sci., 2014), Fisher et al (Atmos. Chem. Phys., 2008), Esler & Scott (J. Atmos. Sci., 2005), Konopka et al (J. Atmos. Sci., 2005), Varotsos (Environ. Sci. Pollution Res., 2002, 2003, 2004) and Allen et al (Geophys. Res. Lett., 2003). In addition to these, I feel that it is imperative that there be comparisons (or relevant discussions) with the paper by Santitissadeekorn et al (Phys. Rev. E, 2010) which provides a Lagrangian analysis and provides pictures very similar to Figure 4. ?*

The SPV breakdown in September 2002 has been extensively studied in the literature using ERA-Interim data and these references are now quoted in the manuscript. A novelty of our study is trying to understand the breakdown and its previous stages in a simple model that shows that the breakdown is related to wave propagation phenomena. The Lagrangian analysis of the breakdown exhibits what are the transport implications of the breaking, showing that the splitting leads to no mass transfer between the two vortices.

The paper by Santitissadeekorn et al (Phys. Rev. E, 2010) presents an interesting approach to estimating the three-dimensional location of the vortex. the promise of this approach is demonstrated by examination of the period from August 1 to September 31 in 1999. (The similarity of pictures during different final warming events can be expected from the similarity in evolution reported by Mechoso et al. (1988). Our paper focuses on a different year (2002) and our concerns are not on the precise location of the polar vortex edge. Therefore, we will keep the paper the paper by Santitissadeekorn et al (Phys. Rev. E, 2010) in mind for future studies, but shall not include a reference in the text.

2. *The term Hyperbolic Trajectories (HTs) is used often in this paper, and described briefly in the introduction. The ideas and intuition given in the third paragraph of the introduction are however only valid in infinite-time flows. There are sometimes additional limitations of steadiness: the cats-eyes structures in these models depends on drawing streamfunction contours (either in the steady frame or in a moving frame), and so are associated with steady situations. While the remainder of the discussion does not necessarily confine itself to steadiness, as far as I am aware, hyperbolic trajectories can only unambiguously be defined for infinite-time situations, using the ideas of exponential dichotomies. The paper by Ide et al (Nonlin. Proc. Geophys., 2002), for example, cites the exponential dichotomy definition but this cannot be adequate for finite-time flows since the variational equation associated with any trajectory will obey the exponential decay requirement by choosing a suitably large prefactor. There have been attempts to fix this: by choosing a prefactor of 1 (Doan et al (J. Differential Equations, 2012), Karrasch (J. Differential Equations, 2013), Duc & Seigmind (Int. J. Bifurc. Chaos, 2008)), or by extending to infinite-times in some fashion (Balasuriya, (J. Nonlin. Sci., 2016)). In general, it seems that HTs are ill-defined for finite-time flows. Throughout the paper, however, the authors seem to be using saddle-like locations of the LD field as their method of identifying HTs. I understand why such locations can be called hyperbolic, but there does not seem to be any justification in calling them trajectories since it is not at all clear if by following these in a time-varying way by computing LDs over a range of t_0 values, an actual trajectory of the system (5) arises. If the flow is nearly steady, it seems that it might be possible to establish the existence of time-varying saddle-points which are close to an actual (infinite-time) hyperbolic trajectory in some instances (Ide et al (Nonlin. Proc. Geophys., 2002), Balasuriya, (J. Nonlin. Sci., 2016)). But is this necessarily so for this situation, viz. using finite-time data, with moderate unsteadiness, and specifically using LD fields to identify saddle points? If the actual term hyperbolic trajectories is not important to what the authors are doing, then perhaps they should simply call them saddle points of the LD field? But even so, claiming a direct relationship to stable and unstable manifolds which are undefined for finite-time flows seems problematic.*

We have extended the explanations on HTs in the Introduction and in Section 2.2. We provide references that compute and justify the use of HT in finite time data sets and also briefly summarize their content. In section 2.2 we have provided also references and arguments that allow us to refer to the the “saddle-like locations of the LD field” as HTs. We have provided references in Section 2.2 that provide a constructive definition for finite time stable and unstable manifolds. We have also briefly summarized the content of these references in the text.

3. *I have some concern about the centered nature of the definition for M in (6). If requiring to find information on the skeleton of transport at time t_0 using FTLEs/FSLEs/.../variational LCSs, the basic approach is to seed initial values at t_0 . If looking for the analog of the stable manifold at t_0 (i.e., repelling LCSs, ridges of forward-time FTLEs), these needs to be advected in forward time. Similarly, the advection is in backward time if looking for analogs of the unstable manifold. It is this information which tells us about the skeleton at time t_0 . For example, Gaultier et al (J. Marine Sci., 2013; J. Geophys. Res. Oceans, 2014) do this advection in backwards time in order to compare with sea-surface temperature fields at the time t_0 . This is also because the advected scalar field (temperature in their case, whereas in this case it could be temperature, ozone concentration, etc, depending on the specific observable of interest in the SPV) at time t_0 would depend on the advection occurring until the time t_0 . Future times surely cannot have an impact. Therefore, why is the integral in (6) being taken from times $t_0 - \tau$ to $t_0 + \tau$? This seems inconsistent with all other Lagrangian approaches. Moreover, its hard to argue that the SPV knows the future! The pinch-off on September 24 in Figure 4(b), for example, uses velocity data into October.*

In Section 2.2 we have included an explanation about the forward and backward integration time used for M , its relation with FTLE and the convenience of this choice for our study. Our approach is completely consistent with all other Lagrangian approaches, found in the literature.

4. *The authors state that M reveal[s]/highlights Lagrangian coherent structures (page 5, lines 12 and 15). Is there a rigorous justification for this - that M specifically reveals coherent structures which move in a Lagrangian way according to the flow? If so, in what way? I am not able to find it directly in the cited references, though I am unable to get access to the latest article (Loposito et al, 2017) that is still in press. To my knowledge and judgment, a relationship has only been established in heuristic senses (and this is also so for other Lagrangian methods used and advocated by others), and in incredibly simplified test cases. Moreover, the authors talk of stable and unstable manifolds here, but of course these things do not have a proper definition in finite-time flows. I believe that the description here needs to be watered down. The LD field is being used as a heuristic, and there is some evidence that it provides the right understanding.*

There are rigorous justifications that invariant manifolds are aligned with singular features of LDs only for specific examples discussed in Lopesino et al 2015 for discrete dynamical systems and Lopesino et al. 2017 for continuous time dynamical systems. Also, the ability of LDs to highlight invariant sets has been explained, and the tool has been linked to the ergodic decomposition theory.

For geophysical flows Mendoza and Mancho (2010, 2012) have compared and found that numerically computed invariant manifolds systematically are aligned with singular features of M , but in these cases there is not any theorem supporting these facts, just numerical evidence. de la Cámara et al. (2013) show that for similar ERA-Interim fields, singular features of M are aligned with numerically computed stable and unstable manifolds (see their Fig. 2).

These issues are explained now in Section 2.2

5. *The kinematic model requires more justification. Why do the amplitudes of the Fourier modes in the kinematic model have these particular r -dependencies? The $r(r-a)$ in vr is understandable, but why $\exp(-r)$? And why the specific forms chosen for PHI1 and PHI2 ? And why these particular forms of time-dependencies for eps1 and eps2 ? Certain parameter values are used in the simulations why were these chosen? In what way are they consistent with parameter values of the SPV? Since the flow for the kinematic model is unsteady, the pictures of Figure 6 must be drawn at a particular time value t_0 , I guess. What is it? I also have a much more general question regarding the kinematical model: What particular understanding does it give to this situation? It is probably possible to have the LD field display all sorts of crazy behavior by choosing the s in various ways, and so what does this particular model do? Now, if it was possible to argue, for example, that a particular instability arising from this kinematic model led to the SPV breakdown, then that might be interesting.*

Section 4 has been extensively revised to address the issues raised by the referee. In particular, the choice of free parameters in the kinematic model is explained in more detail. Further, the SPV breaking is reproduced by the kinematic model (see figure 8). The times at which specific patterns are achieved are also reported.

6. *I am confused by what the authors are trying to achieve in Section 5. Are they trying to say (page 15, line 11) that their kinematic model can be made dynamically- consistent but inserting their PHI into (14) and (15) but then treating h as unknown, and thereby getting an expression for h ? This can possibly be done (though h will satisfy a PDE which may not be easy to solve), but this is highly artificial. This would be demanding that the topography adjusts to the kinematic model that we insist is a solution. One possibility in which this part of the paper might have value is if the s in the kinematic model were somehow chosen as modes associated with the conservation equation (14) this would be similar to the work of Pierrehumbert (Geophys. Astrophys. Fluid Dyn., 1991). The discussion of the earlier parts of this section also appears to lack relevance. If Q were constant in patches, then complicated dynamics are possible subject to Q 's conservation but this simply amounts to nullifying the dynamical constraint, and adds the extra condition (not talked about here) that the streamfunction needs to be chosen such that (15), for a constant Q , is satisfied. Basically, it is true that the potential vorticity distribution imposes constraints on the Lagrangian motion, which may be an aspect the authors are trying to highlight here. For these, the papers by Brown & Samelson (Phys. Fluids, 1994) and Balasuriya (Nonlin. Proc. Geophys., 2001), which deal with both constant and nonconstant Q , may be relevant. In general, I'm not sure I understand the goals this section, and so it requires some attention.*

Section 5 has been rewritten and an explicit calculation of the forcing h is reported, that achieves the conservation of potential vorticity Q for one of the proposed Ψ . The calculation is illustrated for a simple Q choice but it could be repeated for more realistic Q distributions as far as they are defined as piecewise constant functions.

A Simple Kinematic Model for the Lagrangian Description of Relevant Nonlinear Processes in the Stratospheric Polar Vortex

Victor José García-Garrido¹, Jezabel Curbelo^{1,2}, Carlos ~~Rorberto R.~~ Mechoso³, Ana María Mancho¹, and Stephen Wiggins⁴

¹Instituto de Ciencias Matemáticas, CSIC-UAM-UC3M-UCM. C/ Nicolás Cabrera 15, Campus de Cantoblanco UAM, 28049 Madrid, Spain.

²Departamento de Matemáticas, Facultad de Ciencias, Universidad Autónoma de Madrid, 28049 Madrid, Spain.

³Department of Atmospheric and Oceanic Sciences, University of California at Los Angeles, Los Angeles, California.

⁴School of Mathematics, University of Bristol. Bristol BS8 1TW, UK.

Correspondence to: A. M. Mancho (a.m.mancho@icmat.es)

Abstract. In this work we study the Lagrangian footprint of the planetary waves present in the Southern Hemisphere stratosphere during the exceptional Sudden Stratospheric Warming event that took place during September 2002. ~~The Lagrangian analysis of the transport and mixing processes is carried out in the framework of dynamical systems theory, by means of a Lagrangian descriptor. We seek to describe the Lagrangian skeleton of geometrical structures that lead to filamentation phenomena and the breakdown of~~ Our focus is on constructing a simple kinematic model that retains the fundamental mechanisms responsible for complex fluid parcel evolution, during the polar vortex, ~~and establish its relation with how planetary waves interact. Our approach is based on the construction of a simple kinematic model, inspired~~ breakdown and its previous stages. The construction of the kinematic model is guided by the Fourier decomposition of the geopotential field. ~~We show that this model is capable of reproducing the key Lagrangian features present on the reanalysis data such as the formation of filaments eroding the stratospheric polar vortex and~~ The study of Lagrangian transport phenomena in the ERA-Interim reanalysis data highlights hyperbolic trajectories and these trajectories are Lagrangian objects that are the kinematic mechanism for the observed filamentation phenomena. Our analysis shows that the breaking and splitting of the ~~breakdown of the~~ polar vortex is justified in our model by the sudden growth of a planetary wave and the decay of the axisymmetric flow.

1 Introduction

~~A better understanding of the behavior of fluid parcels is of fundamental importance for studies on the~~ The availability of high-resolution and high-quality reanalysis data sets provides us with a powerful tool for obtaining a detailed view of the space-time evolution of the stratospheric polar night vortex (SPV), which has implications for the geophysical fluid dynamics of the entire earth. The complexity of such a detailed view, however, makes it difficult to extract the physical mechanisms underlying notable transport features in the observed behaviour. The goal of this work is to gain new insights into the fundamental mechanisms responsible for complex fluid parcel evolution, since these lie at the heart of our understanding of the dynamics and chemistry of the stratosphere. ~~This~~ To this end we extract, directly from the data, a simple model with a

stripped-down dynamics in order to directly probe, in a controlled and systematic manner, the physical mechanisms responsible for the key observed transport features of the SPV. Models of this kind, termed “kinematic models” have provided a simple approach for studying Lagrangian transport and exchange associated with flow structures such as meandering jets and travelling waves (Bower, 1991; Samelson, 1992; Malhotra and Wiggins, 1998; Samelson and Wiggins, 2006). Other works have used analytical kinematic models to illustrate phenomena in planetary atmospheres (e.g., Rypina *et al.* (2007); Morales-Juberías *et al.* (2015)). In the present paper, we focus on SPV transport processes associated with filamentation and vortex breaking, of which the dynamical structure is not fully understood.

The importance of an increased understanding of the SPV was dramatically demonstrated by the intense research effort that followed the discovery of the “Antarctic Ozone Hole” phenomenon in the 1970’s (Chubachi, 1984; J.D.Farman *et al.*, 1985; Solomon, 1988). Following decades during which monitoring of ozone in atmospheric columns above Antarctica showed little interannual variability, in situ measurements corroborated by satellite data, revealed that ozone was systematically decreasing in the Antarctic lower stratosphere during the southern spring season. Whilst this was immediately associated with the simultaneous increase in atmospheric pollution by anthropogenic activities, several key questions arose (Solomon, 1999): 1) Why over Antarctica and not over the Arctic since pollution sources are stronger in the northern than in the southern hemisphere? 2) Why in the spring season? and 3) Will ozone depletion extend worldwide? The research demonstrated that indeed, indeed, increased atmospheric pollution was to be blamed for the ozone depletion and identified the participating substances and special mechanisms. The research also demonstrated that the unique atmospheric conditions above Antarctica were responsible for the geographic preference for ozone destruction. In particular, it was shown that the strong circumpolar and westerly flow-SPV characteristic of the southern winter and spring stratosphere (~~hereafter stratospheric polar night vortex, SPV~~) contributed-contributes to isolate the cold polar region, setting up a favorable environment for the special chemistry to act. The new knowledge led to the formulation of international agreements that resulted in a negative answer to question 3) above.

Outside The analysis of transport of fluid parcels outside the region isolated by the SPV, ~~research~~ also showed strong stirring and mixing of the flow. In this “surf zone” (McIntyre and Palmer, 1984) air parcels can travel long distances away from the SPV in an environment where contours of long-lived tracers, such as potential vorticity, can stretch forming complex patterns. In this region, ~~which is referred as the “surf zone”~~, Rossby wave breaking is associated with irreversible deformation that pulls material filaments of the outer edge of the SPV and enhances mixing with the exterior flow (McIntyre and Palmer, 1983, 1984, 1985). Such a process makes the SPV edge a barrier to horizontal transport of air parcels (Juckes and McIntyre, 1987) while continuously eroding and regenerating the SPV edge by filamentation (Bowman, 1993). Polvani and Plumb (1992) and Nakamura and Plumb (1994) examined in an idealized setting the way in which Rossby waves break ejecting SPV material outward. The latter conceived a similar setting in which Rossby waves break also inwards.

Dynamical systems theory ~~applies tools that provide valuable insights for describing this type of behavior in fluid flows. Such tools provides valuable insights into the transport processes described in the previous paragraph.~~ Tools of the theory include the geometrical structures referred to as hyperbolic trajectories (HTs), their stable and unstable manifolds and their intersection in homoclinic and heteroclinic trajectories that provide the theoretical and computational basis for describing the filamentation process. ~~Mancho *et al.* (2006b) discussed the possibility of “transferring” this approach to realistic ocean flows~~

~~produced by models. Bowman (2006) pioneered a similar effort for the stratosphere. de la Cámara *et al.* (2013). A challenge~~
in the application of these concepts to realistic geophysical flows is that while the structures mentioned are defined for
infinite time autonomous or periodic systems, geophysical flows are typically defined as finite-time data sets and are not
periodic. Mancho *et al.* (2006b) addressed this challenge for realistic ocean flows by identifying special hyperbolic trajectories
5 in the finite data set, called distinguished hyperbolic trajectories (DHT), and by computing stable and unstable manifolds as
curves advected by the velocity field. A pioneering effort for identifying HT for the stratosphere was due to Bowman (1993).
McIntyre and Palmer (1983); Bowman (1996); de la Cámara *et al.* (2013) suggested that HTs are ~~representative of~~ responsible
for the cat's eye structures associated with planetary wave breaking at the critical levels, i. e. where the wave phase speed
matches the background velocity (Stewartson, 1977; Warn and Warn, 1978). HTs are at the locations where the cats eyelids
10 meet. Perturbation of the cat's-eyes results in irreversible deformation of material contours, signifying Rossby wave breaking.
de la Cámara *et al.* (2013) and Guha *et al.* (2016) identified HTs both within and ~~without outside~~ the SPV, thus suggesting
that Rossby wave breaking can occur in either of those regions. The former authors worked with reanalysis data, while Guha
et al. (2016) used a dynamical model based on the shallow water equations in which the perturbing waves are produced in a
controlled manner. Therefore, HTs are essential features for tracer mixing both outside and inside the vortex, and for occasional
15 air crossings of the vortex edge.

~~Our goal in the present paper is to identify essential features in the filamentation process associated with the breakdown of~~
~~the SPV during a~~ We focus on the SPV behavior during the major stratospheric sudden warming ~~. We focus on the warming~~
~~event~~ that occurred in the southern stratosphere during September 2002. In this unusual event, the SPV broke down in the
middle stratosphere (~~Meechoso *et al.*, 1988; Manney *et al.*, 2006; Charlton *et al.*, 2006~~). ~~On the basis of reanalysis data and the~~
20 ~~application of a Lagrangian descriptor (LD) known as the function M we identify~~ (~~Meechoso *et al.*, 1988; Varotsos, 2002, 2003, 2004; Allen~~
~~We begin by identifying~~ key Lagrangian features of the flow in reanalysis data fields. Next we build a kinematic model
of the event ~~in order to gain insights on the transport processes occurring in the SPV. Typically kinematic models have~~
~~provided a simple approach for studying Lagrangian transport and exchange associated with flow structures such as meandering~~
~~jets and travelling waves (Bower, 1991; Samelson, 1992; Malhotra and Wiggins, 1998; Samelson and Wiggins, 2006). Other~~
25 ~~works have used simple kinematic models to illustrate phenomena in planetary atmospheres (e.g., Rypina *et al.* (2007); Morales-Juberías *et*~~
~~Our kinematic model is constructed to emulate~~, that emulates the behavior of planetary waves ~~as obtained from the reanalysis~~
~~observed in the~~ data. We show that our model produces strikingly similar transport features to those found in the reanalysis
data, ~~confirming the key role played by the HTs during vortex~~ breakdown and filamentation ~~filamentation and breakdown~~.

The structure of the paper is as follows. Section 2 describes the data and methods ~~used in our analysis~~ we use. Section
30 3 describes the ~~identified propagating planetary~~ waves in the reanalysis data in the year 2002 in the stratosphere at ~~some~~
~~specific selected~~ pressure levels (10hPa) ~~and these are related~~, and we relate these to filamentation phenomena and the polar
vortex breakdown that occurred ~~this in that~~ year. Section 4 reproduces the findings ~~in an ad-hoc obtained with our~~ analytical
kinematical model confirming the role played by the HTs in the 2002 vortex filamentation and breakdown. Section 5 discusses
the consistency of the kinematic model as representative of atmospheric flows that conserve potential vorticity. Finally, in
section 6 we present the conclusions.

2 Data and Methods

2.1 ERA-Interim Reanalysis Data

5 To achieve a realistic representation of the atmospheric transport processes, it is crucial to use a reliable and high-quality dataset. We use in this work the ERA-Interim reanalysis dataset produced by a weather forecast assimilation system developed by the European Centre for Medium-Range Weather Forecasts (ECMWF; Simmons *et al.* (2007)). de la Cámara *et al.* (2013) obtained encouraging results on the suitability of the ERA-Interim dataset for Lagrangian studies of stratospheric motions in their comparison of parcel trajectories on the 475 K isentropic surface (around 20 km) using this dataset and the trajectories of
 10 superpressure balloons released from Antarctica by the VORCORE project during the spring of 2005 (Rabier *et al.*, 2010).

The Era-Interim data [set that we selected for this study](#) is available four times daily (00:00 06:00 12:00 18:00 UTC), with a horizontal resolution of $1^\circ \times 1^\circ$ in longitude and latitude and 60 sigma levels in the vertical from 1000 to 0.1 hPa. The data covers the period from 1979 to the present day (Dee *et al.*, 2011) and it can be downloaded from <http://apps.ecmwf.int/datasets/data/interim-full-daily/levtype=sfc/>. In particular we will use the data for the geopotential height and wind [fields on](#) surfaces of
 15 constant pressure for the period August-September 2002.

The geopotential height Z on constant pressure surfaces p is defined as the normalization to $g_0 = 9.80665 \text{ m s}^{-2}$ (standard gravity at mean sea level) of the gravitational potential energy per unit mass at an elevation s (over the Earth's surface), and has the form:

$$Z(\lambda, \phi, p, t) = \frac{1}{g_0} \int_0^{s(p,t)} g(\lambda, \phi, z) dz, \quad (1)$$

20 where g is the acceleration due to gravity, λ is longitude, ϕ is latitude and z is the geometric height (Holton (2004)). [In the quasi-geostrophic approximation, the geopotential height is proportional to the streamfunction of the geostrophic flow \(Holton, 2004\).](#)

For the analysis of planetary waves, we apply a zonal Fourier decomposition [of to](#) the geopotential height field on the 10 hPa pressure level (approximately 850 K potential temperature). The zonal wave decomposition yields:

$$25 \quad Z = \mathcal{Z}_0(\phi, p, t) + \sum_{k=1}^{\infty} \mathcal{Z}_k(\lambda, \phi, p, t). \quad (2)$$

The mean flow is defined as:

$$\mathcal{Z}_0(\phi, p, t) = \frac{1}{2\pi} \int_0^{2\pi} Z(\lambda, \phi, p, t) d\lambda, \quad (3)$$

and the different modes \mathcal{Z}_k with wavenumber $k \geq 1$ have the sinusoidal description:

$$\mathcal{Z}_k(\lambda, \phi, p, t) = \mathcal{B}_k(\phi, t) \cos(k\lambda + \varphi_k(\phi, p, t)) \quad (4)$$

where $\lambda \in [0, 2\pi)$ is longitude, $\phi \in [-\pi/2, \pi/2]$ is latitude, \mathcal{B}_k is the amplitude of the wave and φ_k its phase. During the warming event occurred in the southern stratosphere during September 2002 the flow was dominated by the contributions of the mean flow and the two longest planetary waves (\mathcal{Z}_1 and \mathcal{Z}_2 ; Krüger *et al.* (2005))

5 2.2 Lagrangian Descriptors

~~The theory of dynamical systems provides an ideal framework for analyzing nonlinear transport and mixing processes that take place in the stratospheric polar vortex by means of Lagrangian techniques. One of the main goals of dynamical systems theory is the~~ Dynamical systems theory provides a qualitative description of the evolution of particle trajectories by means of geometrical objects that partition the phase space (the atmosphere in our case) into regions in which the system shows distinct dynamical behaviors. These geometrical structures act as material barriers to fluid parcels and are closely related to flow regions known as hyperbolic, where rapid contraction and expansion takes place. ~~This methodology has become a cornerstone on the applications of the qualitative theory of dynamical systems to geophysical fluids.~~

Several Lagrangian techniques have been developed in order to ~~describe the Lagrangian coherent structures (LCS) that comprise the skeleton of the flow and govern transport and mixing~~ detect such structures in geophysical fluids. ~~The search for such structures in geophysical contexts~~ This is challenging because ~~in these,~~ while classical dynamical systems theory is defined for infinite time autonomous or periodic systems, in geophysical contexts the velocity fields are generally time-dependent, aperiodic in time, ~~time-dependent~~ and defined over a finite discrete space-time domain. Among other ~~the developed techniques include,~~ techniques developed are finite-size Lyapunov exponents (FSLE) (Aurell *et al.*, 1997), finite-time Lyapunov exponents (FTLE) (cf. Haller (2000); Haller and Yuan (2000); Haller (2001); Shadden *et al.* (2005)). ~~The techniques also~~ Other techniques include distinguished hyperbolic trajectories (DHT) (~~Ide *et al.*, 2002; Ju *et al.*, 2003; Madrid and Mancho, 2009~~) (Ide *et al.*, 2002; Ju *et al.*, 2003), the direct calculation of manifolds as material surfaces (~~Mancho *et al.*, 2003, 2004~~) (Mancho *et al.*, 2003, 2004, 2006b), the geodesic theory of LCS (Haller and Beron-Vera, 2012) and the variational theory of LCS (Farazmand and Haller, 2012), etc. Our choice in this work will be the use of the Lagrangian Descriptor (LD) function M introduced by Madrid and Mancho (2009); Mendoza The function M has been applied in a variety of geophysical contexts. For example, in the ocean it has been used to analyze the structure of the Kuroshio current (Mendoza and Mancho, 2012), to discuss the performance of different oceanic datasets (Mendoza *et al.*, 2014), to analyze and develop search and rescue strategies at sea (Garcia-Garrido *et al.*, 2015), and to manage efficiently in real-time the environmental impact of marine oil spills (Garcia-Garrido *et al.*, 2016). In the field of atmospheric sciences, M has been used to study transport processes across the Southern SPV and RWB by de la Cámara *et al.* (2012, 2013); Smith and Mancho (2014) and to investigate the Northern Hemisphere major stratospheric final warming in 2016 (Manney and Lawrence, 2016).

30 The dynamical system that governs the atmospheric flow is given by:

$$\dot{\mathbf{x}} = \mathbf{v}(\mathbf{x}(t), t) \quad , \quad \mathbf{x}(t_0) = \mathbf{x}_0 \quad , \quad (5)$$

where $\mathbf{x}(t; \mathbf{x}_0)$ represents the trajectory of a parcel that at time t_0 is at position \mathbf{x}_0 , and \mathbf{v} is the wind velocity field. Since our interest is in the time scale of stratospheric sudden warmings (~ 10 days) we can assume to a good approximation that the fluid parcels evolve adiabatically. Therefore trajectories are constrained to surfaces of constant specific potential temperature (isen-

tropic surfaces). We will concentrate on the 850 K surface, which is in the middle stratosphere and approximately corresponds to the 10 hPa levels. In section 3 we expand on the reasons for this choice.

To compute fluid parcels trajectories it is necessary to integrate (5). As the velocity field is provided on a discrete spatio-temporal grid, the first issue to deal with is that of interpolation. We use apply bicubic interpolation in space and third-order Lagrange polynomials in time (see Mancho *et al.* (2006a) for details). Moreover for the time evolution we have used an adaptive Cash-Karp method. It is important to remark that as done in (de la Cámara *et al.*, 2012) for the computation of particle trajectories we use cartesian coordinates in order to avoid the singularity problem arising at the poles from the description of the Earth's system in spherical coordinates.

Our choice of LD is the function M introduced in Madrid and Mancho (2009); Mendoza and Mancho (2010, 2012). The M function is defined as follows:

$$M(\mathbf{x}_0, t_0, \tau) = \int_{t_0 - \tau}^{t_0 + \tau} \|\mathbf{v}(\mathbf{x}(t; \mathbf{x}_0), t)\| dt, \quad (6)$$

where $\|\cdot\|$ stands for the modulus of the velocity vector. At a given time t_0 , the function $M(\mathbf{x}_0, t_0, \tau)$ measures the arc length traced by the trajectory starting at $\mathbf{x}_0 = \mathbf{x}(t_0)$ as it evolves forwards and backwards in time for a time interval τ . Sharp changes of M values (what we call singular features of M) occur in narrow gaps for sufficiently large τ , for very close initial conditions and highlight stable and unstable manifolds (repelling and attracting LCS) and, at their crossings, hyperbolic trajectories. A thorough explanation of how

Mendoza and Mancho (2010, 2012) have performed systematic numerical computations of invariant manifolds and found that they are aligned with singular features of M highlights manifolds discussed in (Mendoza and Mancho, 2010; Mancho *et al.*, 2013; Lopez and Mancho, 2015). The capability. They also provide examples in geophysical flows where manifolds are defined in a constructive way. Invariant manifolds are mathematical objects classically defined for infinite time intervals. The unstable (stable) manifold of a hyperbolic fixed point or periodic trajectory is formed by the set of trajectories that in minus (plus) infinity time approach these special trajectories. In geophysical contexts this definition is not realizable, because only finite time aperiodic data sets are possible. Nevertheless, manifolds can still be defined constructively with the following procedure. At the beginning time, these curves are approximated by segments with short length, aligned with the stable and unstable subspaces of the DHT identified with algorithms described in Ide *et al.* (2002); Madrid and Mancho (2009). This starting step aims to build a finite-time version of the asymptotic property of manifolds. Next segments are advected forwards and backwards in time by the velocity field. Due to the large expansion and contraction rates in the neighbourhood of the DHT, the curves grow rapidly in forwards and backwards time and specific issues are addressed by the procedure described in (Mancho *et al.*, 2003, 2004). The procedure provides curves, manifolds, that by construction are barriers to transport in geophysical flows. In this way since manifolds are aligned with singular features of M and its generalizations (Lagrangian Descriptors) for revealing Lagrangian coherent structures was extensively analyzed and tested in, the latter belong to invariant curves of the system (5), and therefore their crossing points are indeed trajectories of the system (5). The capability of LDs in general, and M in particular, for revealing invariant manifolds was analyzed in detail in Mancho *et al.* (2013). Lopesino *et al.* (2015) and Lopesino *et al.* (2017) have recently established

~~a rigorous mathematical foundation (in specific examples) for LDs in discrete and time continuous~~ discussed, in discrete
5 ~~and continuous time~~ dynamical systems, respectively, ~~and highlighted the underlying connections with the classical theory of~~
~~dynamical systems. Lagrangian descriptors have been applied in a variety of geophysical contexts. For example, in a theoretical~~
~~framework for some particular versions of LDs in specific examples.~~

The consistency between the output field of Eq. (6) and FTLE ridges has been discussed in some references (see Mendoza and Mancho (2012)).
The integral expression in Eq. (6) can be split in two terms: one for forwards time and other for backwards time integration.
10 Explicit calculations discussed in Mancho *et al.* (2013) for a linear saddle, show that singular features of the first term are
aligned with the stable manifolds while those for the backwards time integration are aligned with the unstable manifolds. This
is similar to what is obtained with FTLE that highlight stable and unstable manifolds, respectively for forwards and backwards
time integration intervals. The fact that we choose to add both fields is advantageous for highlighting hyperbolic trajectories at
the crossing points of the ~~ocean they have been used to analyze the structure of the Kuroshio current (Mendoza and Mancho, 2012),~~
15 ~~to discuss the performance of different oceanic datasets (Mendoza *et al.*, 2014), to analyze and develop search and rescue~~
~~strategies at sea (Garcia-Garrido *et al.*, 2015) and also to manage efficiently in real time the environmental impact of marine~~
~~oil spills (Garcia-Garrido *et al.*, 2016). In the field of atmospheric sciences, LDs have been used to study transport processes~~
~~across the Southern SPV and RWB by de la Cámara *et al.* (2012, 2013); Smith and McDonald (2014); Guha *et al.* (2016) and~~
~~to investigate the Northern Hemisphere major stratospheric final warming in 2016 (Manney and Lawrence, 2016)~~ singular
20 ~~features.~~

As an example relevant to the case that motivates the present study, we show in Fig. 1 the evaluation of M over the Southern
Hemisphere using $\tau = 15$ on the 850 K isentropic level for the 5th August 2002. The representation shows a stereographic
projection (see Snyder (1987)) in which the SPV is clearly visible by the bright yellow color, and also the filamentation
phenomena ejecting material both from the outer and inner part of the jet. These filaments are related to the presence of
25 hyperbolic trajectories highlighted in the figure. ~~All figures presenting~~ The fact that these saddle points of the LD field are
hyperbolic trajectories of the system (5) is numerically supported. To this end de la Cámara *et al.* (2013) show that (see their
Fig. 2), for similar ERA-Interim fields, these points belong to the intersection of stable and unstable manifolds highlighted
by the singular features of the field. In what follows, all figures showing M ~~in what follows~~ were computed with $\tau = 15$. This
choice of τ is made based on the fact that diabatic heating/cooling processes in the extratropical stratosphere generally have
30 longer time scales than those of horizontal advection. Hence, air parcels move on two-dimensional isentropic surfaces to a
good approximation (they stay within 850K for 30 days (Plumb, 2007). Moreover, diabatic heating rates in the Antarctic mid
stratosphere are on the order of 0.5 K day^{-1} , although uncertainties in this magnitude remain large (Fueglistaler *et al.*, 2009).
During the time interval of our calculations of isentropic trajectories ($\tau = 15$ days, i.e. time period of 30 days), the material
surface would experience an increase of potential temperature of around 15 K. Nevertheless, calculations of M using wind
fields at 850 K and 700 K (not shown) produce qualitatively similar results. This suggests that horizontal motions of the parcels
will be affected by similar geometric structures at those isentropic levels and that the isentropic approach is justified in our
problem.

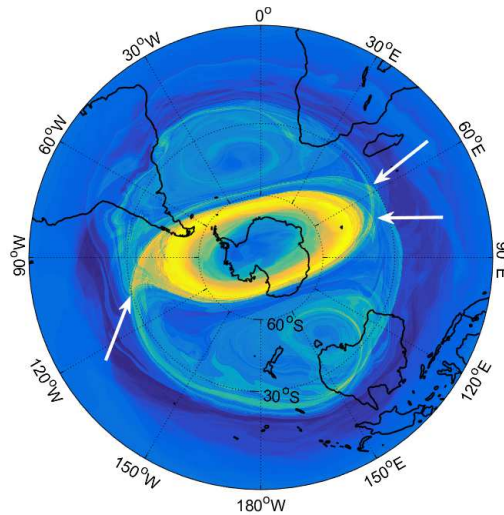


Figure 1. Stereographic projection of Lagrangian descriptors evaluated using $\tau = 15$ on the 850 K isentropic level for the 5th August 2002 at 00:00:00 UTC. The SPV is clearly visible as well as three hyperbolic trajectories (HTs) outside the vortex (marked with white arrows), two northeast and one southwest of it. Filamentation phenomena, which occurs in the neighborhood of HTs, is visible both inside and outside the vortex, where the outer filamentous structures play the role of eroding the jet barrier. Notice also the presence of two eddy coherent structures ~~above and below over~~ the SPV South Atlantic and south of Australia.

5 3 Data Analysis

As we ~~explained~~ indicated in the previous section, in order to characterize the planetary waves that propagate in the stratosphere we carry out a Fourier decomposition of the geopotential height. In Fig. 2 we show the axisymmetric mean-flow ~~and together~~ with waves 1 and 2 in the geopotential field for the 22nd September 2002 on the 10 hPa pressure surface. The time evolution of these waves is ~~also~~ described in the supplementary movies S1-S4. Animations S1-S3 ~~contain simulations of~~ show components 0, 1 and 2 separately for the time period of interest, ~~and while~~ S4 shows the ~~evolution of the three waves~~ summed superposition of these three waves. It is important to ~~remark~~ reiterate that, since the geopotential provides a good approximation of the streamfunction of the large-scale flow in the extratropical regions (~~see e.g. Holton (2004)~~), its analysis will ~~help us to build in~~ the next section a provide us with guidance on the building of the simple kinematic model presented in the next section.

On the 10 hPa pressure level, the winter SPV in the Southern Hemisphere ~~is defined by~~ can be broadly defined as a circumpolar westerly jet. ~~During September 2002, this circulation was severely disrupted in the middle stratosphere. Figure~~ Figures 3a) illustrates this disruption by showing a time series of the amplitude of the axisymmetric Fourier component (see figure 2b)) of the geopotential height along a chosen longitude (as it is axisymmetric all longitudes provide the same output). This component is the most representative of the flow. In the quasi-geostrophic approximation, the latitudinal gradient of this component approximates the zonal mean velocity (Holton, 2004). The time series in figure 3a) shows that in the neighbourhood

5 of the South Pole (between latitudes -65 to -90) this gradient changes sign around the 22nd of September 2002, indicating a reversal of the zonal meanflow.

and 3b) illustrate the evolution of the circulation during August-September 2002. We can clearly see the gradual deceleration of the SPV and the abrupt change in direction from westerly to easterly velocities at high latitudes that occurred on 22 September. This was a unique major SSW in the southern stratosphere. Planetary waves in the southern stratosphere were very active during the period where the 2002 SSW developed. Fig. 3 b) illustrates the time evolution c) presents a time series of the ratio between the amplitudes of waves 1 and 2. Increased wave 1 amplitude results in a displacement of the SPV vortex from a circumpolar configuration, while increased wave 2 results in a stretching the SPV in one direction and contraction (or "pinching") in the orthogonal direction. According to Fig. 3 b,c), the amplitude of wave 1 was generally larger than that of wave 2 during the entire period, confirming the major role of this wave. Finally, Fig. 3 d) displays the variations in time of the ridges of wave 1 and wave 2. Note that wave 1 is quasi-stationary, while wave 2 propagates eastward as is typical in the southern stratosphere during early spring (Manney *et al.*, 1991; Quintanar and Mechoso, 1995).

The contribution of these different waves to the evolution of the SPV and their transport implications is clearly observed in movie S5. A regime giving rise to the stretching of material lines and the appearance of hyperbolic regions and the associated filamentation processes is observed. These filamentous structures and HTs are clearly highlighted by the application of LDs to the wind fields, as shown in Figs. 1 and 4. Filamentation phenomena occurs both inside and outside the vortex, where the outer filamentous structures play the role of eroding the jet material barrier. Also, the presence of HTs in the flow (see captions of Figs. 1 and 4) indicate regions subjected to intense deformation and mixing (see Ottino (1989)). It is important to highlight We emphasize that HTs appear both inside and outside the SPV. Finally, the breakup of the SPV on the 24th September 2002 depicted in Fig. 4 b) (see also animation S5) is caused by the formation of a HT in the interior of the vortex whose manifolds occurs when manifolds associated with an HT that forms within the SPV connect the interior and the exterior of the jet, allowing for the interchange of air parcels through the barrier. The pinching of the SPV takes place off the pole since the intensity of because Z_1 is dominant has large amplitudes in the days preceding the breakup. As we approach the 24th September, Z_2 becomes of the same order as Z_0 , and the jet elongates and flattens. At this point, the mean flow reversal is crucial for completing the pinching process and the appearance of a HT in the interior of the vortex which splits it as this splits apart.

4 The kinematic model

Kinematic models have a long history in the geophysical fluid dynamics community. They allow for a detailed parametric study of the influence of identified flow structures on transport and exchange of fluid parcels. All early studies utilizing the dynamical systems approach for understanding Lagrangian transport and exchange associated with flow structures such as meandering jets and travelling waves have employed kinematic models. A review of this earlier work, can be found in Samelson and Wiggins (2006) (see Samelson and Wiggins (2006)).

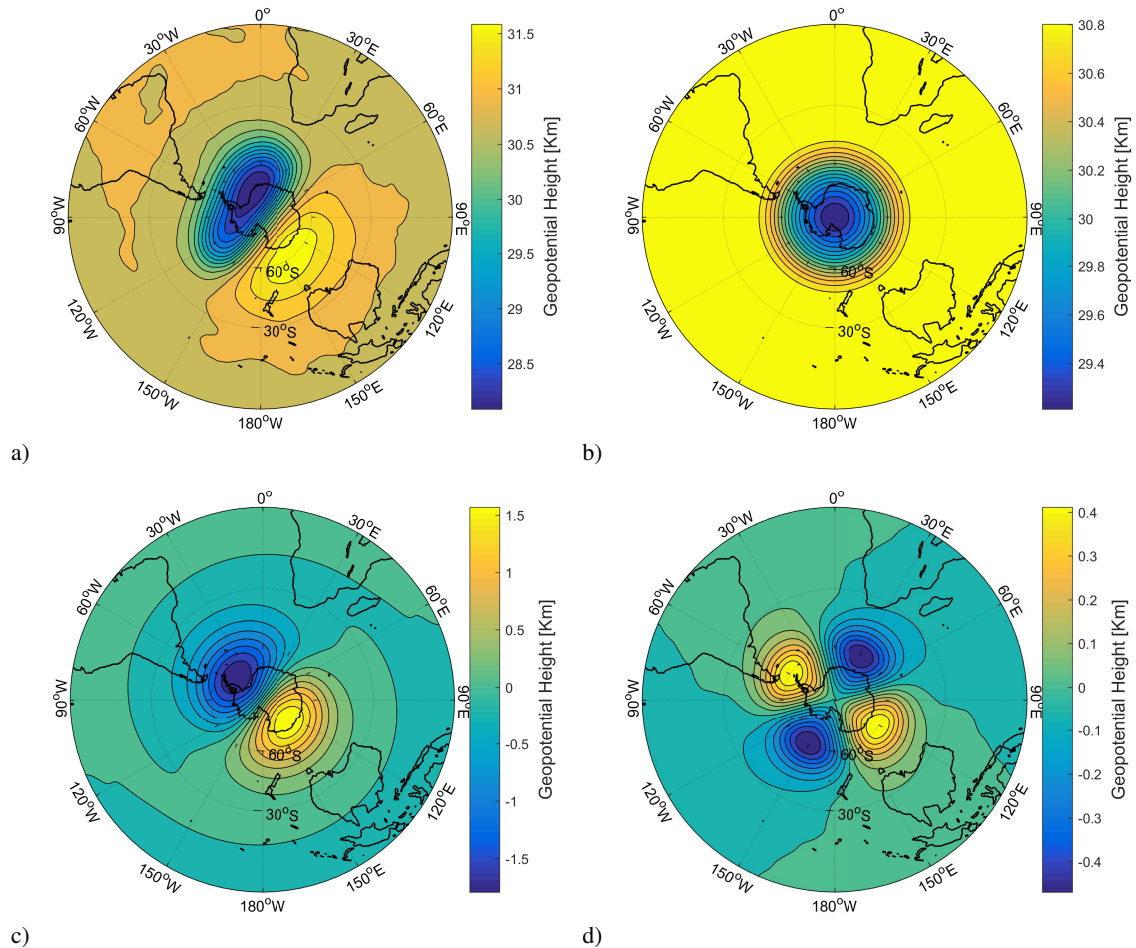


Figure 2. Stereographic projection of the geopotential height field and its Fourier decomposition for the 10 hPa pressure level on the 22nd September 2002 at 00:00:00 UTC: a) Geopotential height; b) Mean flow; c) Fourier component Z_1 ; d) Fourier component Z_2 . Observe how the amplitude of the planetary wave with wavenumber 1 energetically dominates Z_2 , since its amplitude is can be at least three times larger than that of wavenumber 2.

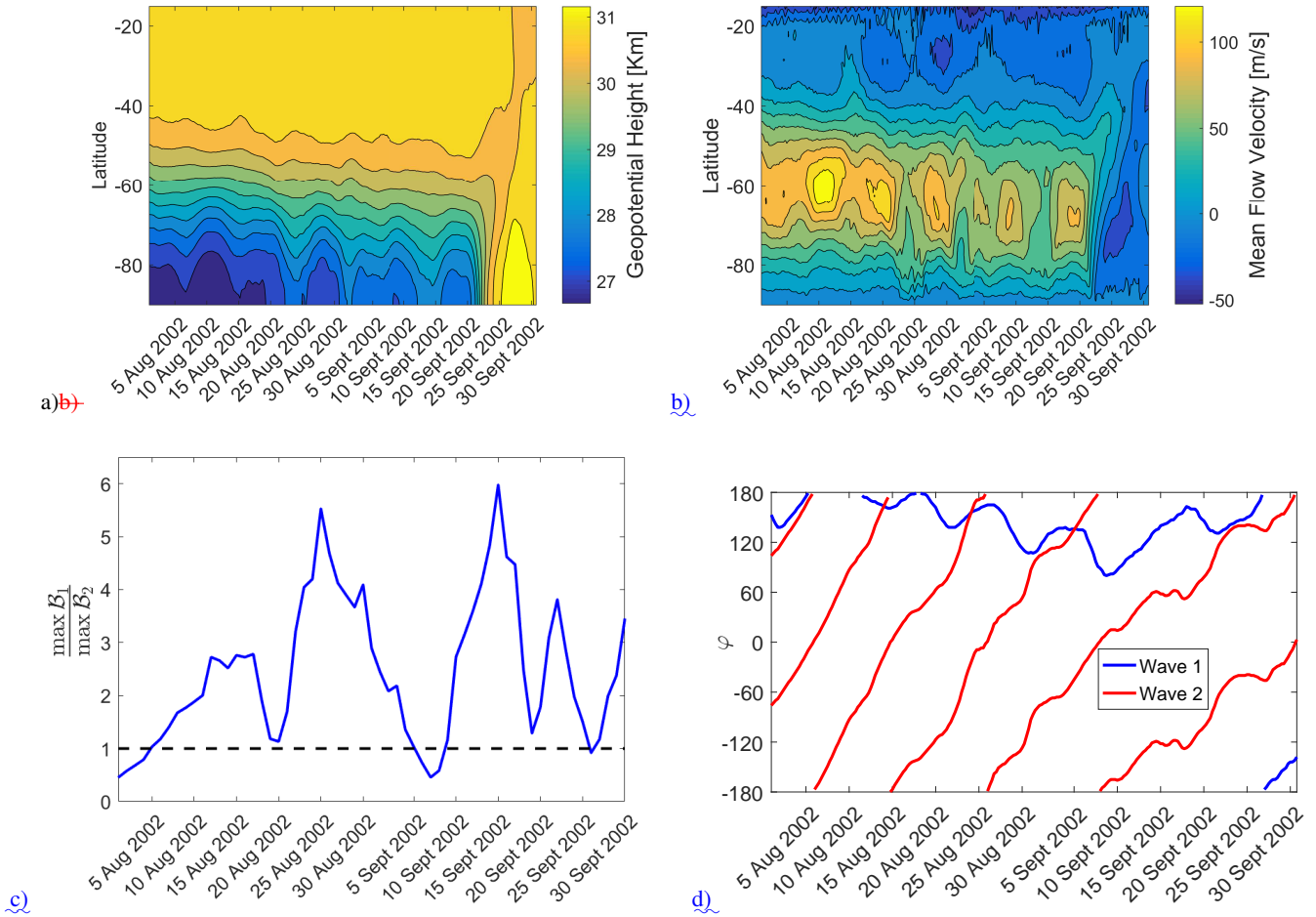


Figure 3. On the 10 hPa pressure level: a) Time evolution of the geopotential height corresponding to the mean flow measured along a meridian. b) Time evolution of the mean flow velocity. Notice the change in wind direction from westerly to easterly that takes place from the 22nd to the 24th of September 2002 giving rise to the pinching of the SPV. c) Time series of the ratio of the maximum amplitudes of Rossby waves 1 and 2. It is important to remark how d) Hoymöller (time-latitude) showing the component 1 clearly dominates component 2 throughout most position of the period ridges of waves 1 and 2 at latitude 60°S.

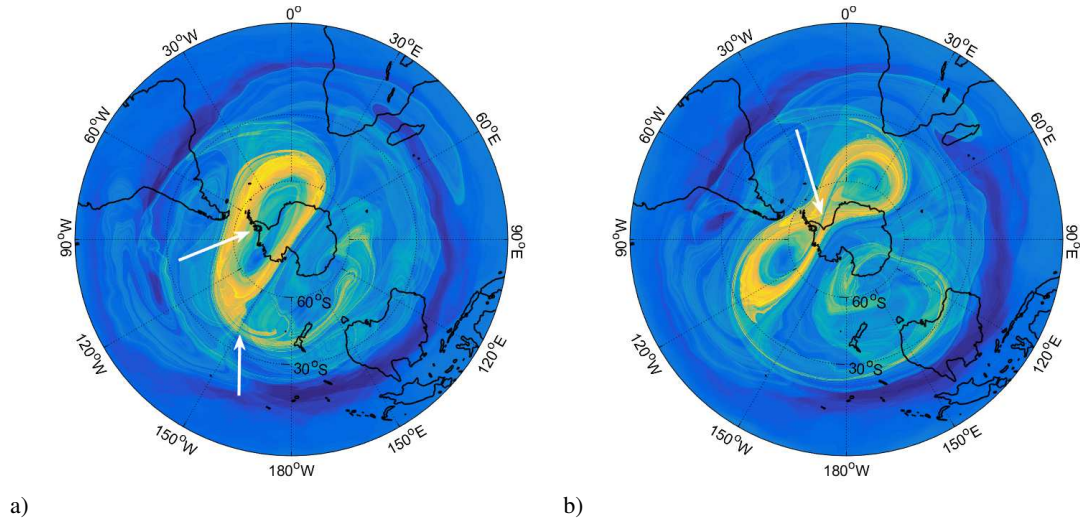


Figure 4. Stereographic projection of the M function calculated using $\tau = 15$ on the 850 K isentropic level for the: a) 22nd September 2002 at 00:00:00 UTC; b) 24th September 2002 at 00:00:00 UTC. Filamentation phenomena and hyperbolic trajectories (marked with white arrows) are nicely captured in these simulations both in the exterior and the exterior of the SPV. Observe how the breakdown-of-the-vortex-breakdown on the 24th September occurs via-when, in the appearance-interior of an-hyperbolic-point-inside-the polar-jet-which-vortex, a HT allows the transport and mixing of air-parcels across the coherent-barrier.

~

Continuing in this spirit, in-this-section we propose a kinematic model that allows us to identify in a controlled fashion, the characteristics of the distinct propagating waves that are responsible for the different Lagrangian features observed in the SPV. Our kinematic model is inspired by the Fourier component decomposition of the geopotential extracted from the ECMWF ERA Interim data as discussed in the previous section. The analysis of data from August and September 2002 shows a mean axisymmetric flow, disturbed mainly by waves with planetary wavenumbers 1 and 2 whose amplitudes and phase speeds vary in a time-dependent fashion.

Therefore we propose a kinematic model in the form of a streamfunction that-is-the-sum-of-the-first-three-Fourier-components of-the-geopotential-field: given by,

$$\Psi = \varepsilon_0 \Psi_0 + \varepsilon_1 \Psi_1 + \varepsilon_2 \Psi_2, \quad (7)$$

where $\varepsilon_0, \varepsilon_1, \varepsilon_2$ are the perturbation parameters, which we will refer to as amplitudes, and Ψ_i are the Fourier components along the azimuthal direction with wavenumbers $i = 0, 1, 2$ respectively, which we describe next.

The-streamfunction-is-defined-on-a-horizontal-We-will-work-in-a-plane (x, y) that is the orthographic projection of the Southern hemisphere-Hemisphere onto the equatorial plane (cf. Snyder (1987)). For simplicity, and in order to highlight the periodicity along the azimuthal direction, the components of the streamfunction are given in terms of polar coordinates satis-

10 flying $x = r \cos(\lambda)$ and $y = r \sin(\lambda)$ where the azimuthal direction λ is related to the geographical longitude and r is related to the geographical latitude.

The mean axisymmetric flow is given by:

$$\Psi_0 = e^{-r}(ar + a - r(r + 2) - 2)$$

15 where a is a tunable constant that is varied to represent different phenomena. This component of the streamfunction has been computed by modeling the velocity in the azimuthal direction as $v_\lambda = r(r - a)e^{-r}$ and then integrating particular forms of Ψ_0 , Ψ_1 and Ψ_2 are inspired by the Fourier decomposition of the geopotential field shown in figure 2 for the 10hPa pressure level on the 22nd September 2002. Starting with the mean zonal velocity, we will assume a jet with the following expression

$$v_\lambda = r(r - a)e^{-r}. \quad (8)$$

20 Therefore, $v_\lambda = 0$ only at $r = 0$ and $r = a$, and the velocity decreases exponentially away from the pole. Changing the values of a will allow us to consider variations in the position of the jet maxima. Integration with respect to r gives,

$$\Psi_0 = e^{-r}(ar + a - r(r + 2) - 2), \quad (9)$$

The other streamfunction components are:

$$\Psi_1 = -r^2 e^{-r^2} \sin(\lambda) \quad (10)$$

and

$$\Psi_2 = (r/d)^2 e^{-r^2/d} \sin(2\lambda + \omega_2 t + \pi/4). \quad (11)$$

where d is also a tunable constant. A representation of the Fourier components of the streamfunction is given in figure 5.

5 The components Ψ_1 and Ψ_2 typically are time dependent because they are waves that propagate ω_2 are also tunable constants, and the phase $\pi/4$ was added so that the relative positions of the waves 1 and 2 at $t = 0$ resemble those in figure 2. Positive values of ω_2 correspond to clockwise rotation. Note that (11) can represent a wave that propagates in the azimuthal direction λ . In our setting we just consider the propagation of wave two, thus expression (11) is rewritten as follows: if ω_2 is different than zero. Figure 5 shows the streamfunctions (9), (10) and (11) in the horizontal plane for the particular set of parameters indicated in the corresponding caption. In the panels of figure 5 and following, the center represent the South Pole and the circular dashed line indicates the Equator. The similarity between figure 2 and 5 for the selected set of parameters is evident taking into consideration that they correspond to stereographic and orthographic projections, respectively.

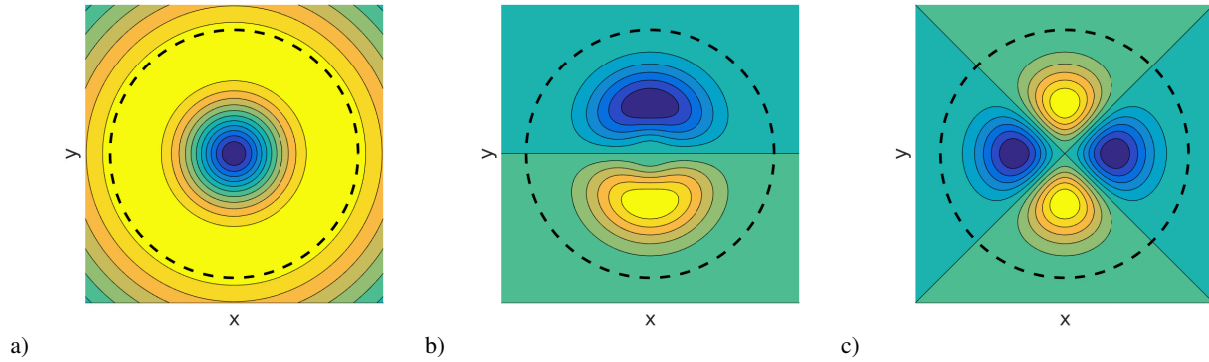


Figure 5. Representation of the three components of the streamfunction. a) $\varepsilon_0 \Psi_0$, for $a = 2$ and $\varepsilon_0 < 0$; b) Ψ_1 ; and c) Ψ_2 for $d = 1, w_2 = 0$.

$$\Psi_2 = (r/d)^2 e^{-r^2/d} \sin(2(\lambda + 2\omega_2 t)).$$

The velocity of fluid parcels in the Cartesian coordinates (x, y) is given by Hamilton's equations:

$$\frac{dx}{dt} = -\frac{\partial \Psi}{\partial y}, \quad \frac{dy}{dt} = \frac{\partial \Psi}{\partial x} \quad (12)$$

Additionally the amplitudes ε_1 and ε_2 are time dependent as they switch on and off the presence of each wave. We take the amplitudes to be time dependent in order to emulate changes in magnitudes. Let us start with ε_0 constant and,

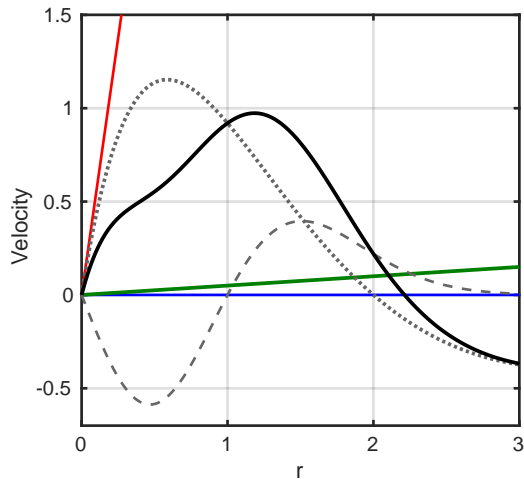
$$\varepsilon_1 = \eta_1(1 + \sin(\mu t + \pi)), \quad \varepsilon_2 = \eta_2(1 + \sin(\mu t)). \quad (13)$$

Here η_1 and η_2 are constants. The time dependence of ε_1 and ε_2 allows us to analyze each wave either separately or together and their transient effect on the observed Lagrangian structures and therefore their transport implications. The time dependence in (13) is such that one amplitude decreases when the other increases, roughly allowing conservation of the total energy when both waves are present. In the simulations presented below $\mu = 2\pi/10$.

The equations of motion for fluid parcels in the Cartesian coordinates (x, y) are given by Hamilton's equations:-

$$\frac{dx}{dt} = -\frac{\partial \Psi}{\partial y}, \quad \frac{dy}{dt} = \frac{\partial \Psi}{\partial x}$$

Figure 7 summarizes the Lagrangian findings obtained from the kinematic model with different parameters. Figures 7 a) and b) highlight a jet which in We begin by considering the case of a mean flow with $a = 2$ and just wave 2 rotating at different



a) ~~b) c) d)~~

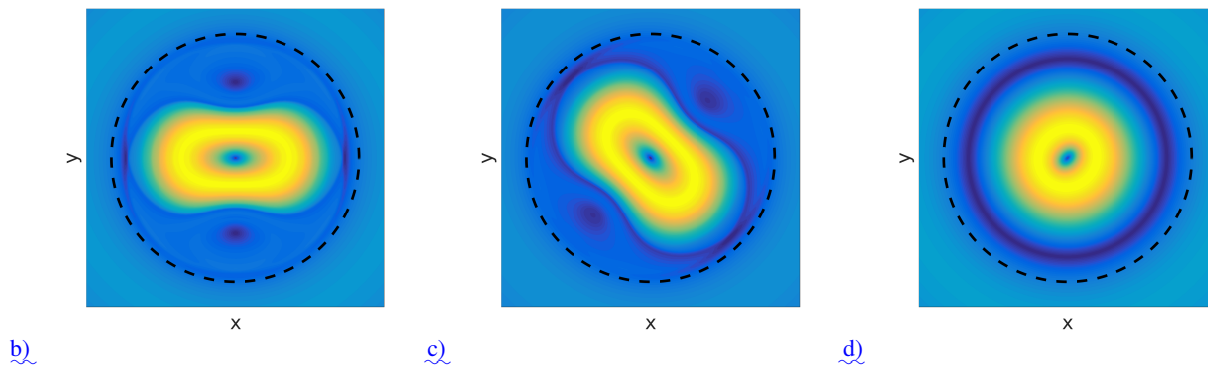


Figure 6. Some illustrative parameter choices for the kinematic model. a) A representation of the mean flow azimuthal velocity (dotted line), the azimuthal velocity of wave 2 for the stationary case along $\lambda = 0$ (dashed line), the total azimuthal velocity along $\lambda = 0$ (solid line), the phase velocity for $\omega_2 = 0.1$ (green line) and the phase velocity for $\omega_2 = 4\pi$ (red line); b) representation of the M function for a kinematic model considering a mean flow ($a = 2$) plus a stationary wave 2 ($d = \eta_2 = 1$); c) the same as b) for a rotating wave 2 with $\omega_2 = 0.1$; d) the same as b) for a rotating wave 2 with $\omega_2 = 4\pi$.

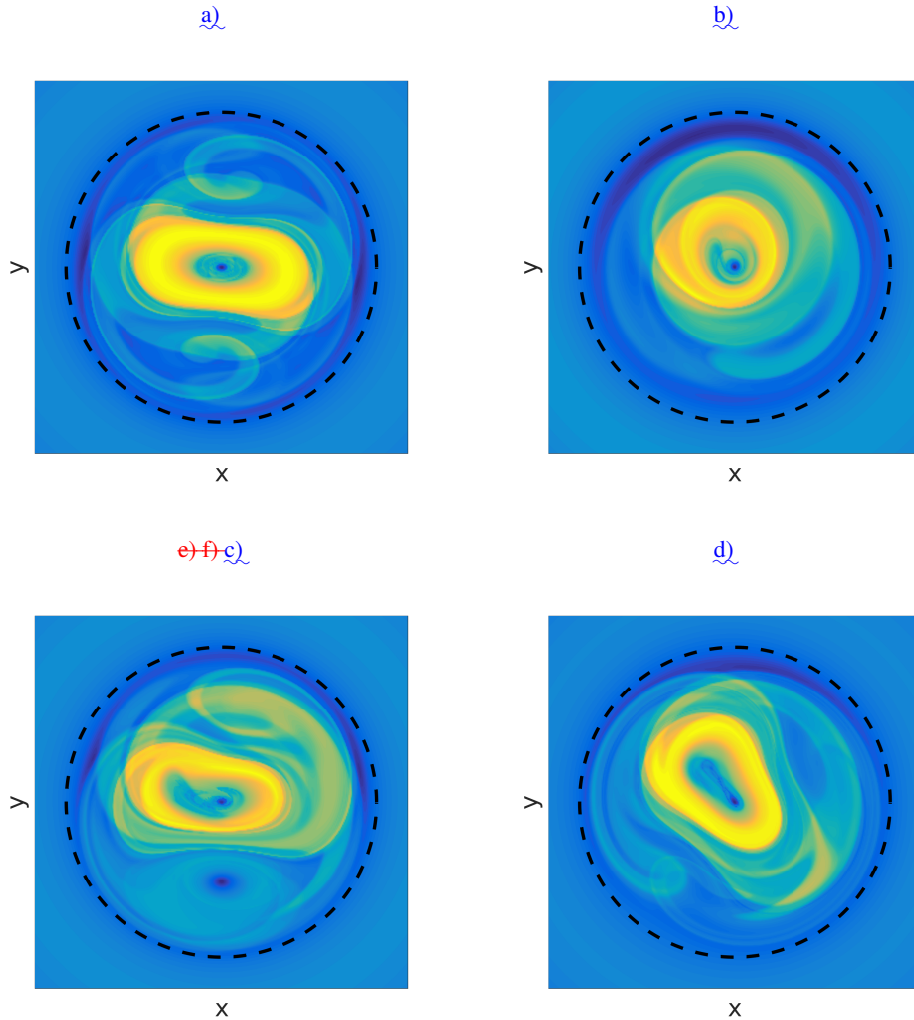


Figure 7. Lagrangian patterns obtained for $\tau = 15$ and different parameter settings in the kinematic model. a) ~~The model keeps Ψ_0 and Ψ_1 adjusted to perturb the vortex in its interior part;~~ b) ~~the model keeps Ψ_0 and Ψ_2 adjusted to perturb the vortex in its interior part;~~ c) Fourier components Ψ_0 and Ψ_1 ~~Ψ_2~~ the latter adjusted to perturb the vortex in its outer part; ~~d) Fourier components Ψ_0 and Ψ_2 Ψ_1 the latter adjusted to perturb the vortex in its outer part;~~ ~~e) the model keeps Ψ_0 , Ψ_1 and Ψ_2 ;~~ ~~f) d) the model keeps Ψ_0 , Ψ_1 and Ψ_2 with parameters adjusted differently to e);~~

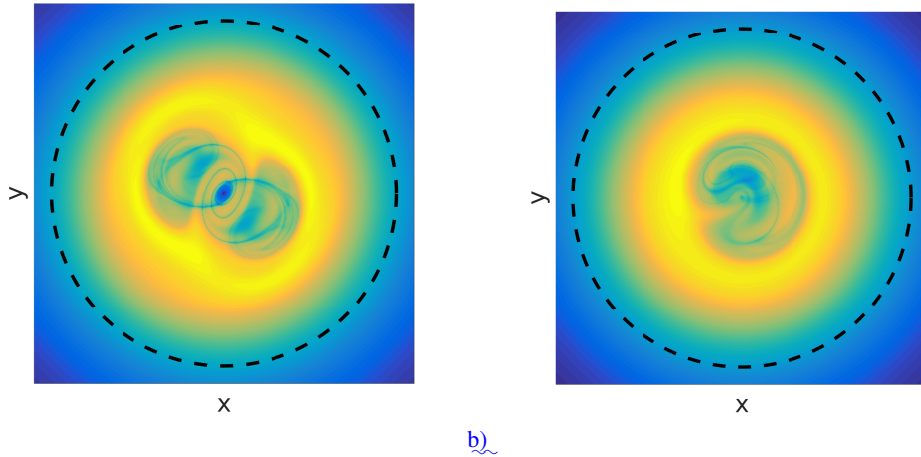


Figure 8. Lagrangian patterns obtained for $\tau = 15$ and different parameter settings in the kinematic model. a) the model keeps Ψ_0 and Ψ_2 adjusted to perturb the vortex in its interior part; b) The model keeps Ψ_0 and Ψ_1 adjusted to perturb the vortex in its interior part.

speeds. Furthermore $d = 1$ and $\eta_2 = 1$. Let us start with $\omega_2 = 0$, i.e. the stationary case. For this case, the dotted line in figure 6a) shows the azimuthal velocity of the mean flow for $\varepsilon_0 = -2.5$, the dashed line is the azimuthal velocity of wave 2 at $\lambda = 0$, where the radial velocity cancels, the interior is eroded, respectively, by the presence of perturbing waves with wave numbers 1 or 2. In a) the parameters switch on a transient amplitude for wave 1 ($\eta_1 = 1, \eta_2 = 0$) on an axisymmetric flow where $\varepsilon_0 = 2.5$ and $a = 0.5$. Lagrangian structures are obtained from the function—solid line is the total azimuthal velocity and the blue line is the wave phase speed. According to figure 6a) there are two points where the total velocity cancels, one being the origin. We can also easily see that there are additional fixed points at the r coordinate where the dotted and dashed curves intersect, but placed along the lines $\lambda = \pi/2, 3\pi/4$. This gives a total of five points in the hemisphere. Figure 6 b) shows the M function for $\tau = 15$. A protruding material filament from the interior—evaluated on this stationary field at $t = 0$. The minima of M highlighting the five fixed points are evident. Moreover, we can see two hyperbolic points in the outer part of the vortex is observed, which is related to the presence of one hyperbolic trajectory. In b) parameters switch on a transient amplitude for a traveling.

Next we consider the case with the same parameters except for ω_2 . Figure 6 c) shows how this picture changes when $\omega_2 = 0.1$, i.e. for slow rotation rate of wave 2. The total azimuthal velocity of the wave, in this case, is given by the dashed line in figure 6a) plus the phase velocity represented by the green line in the figure. If this total azimuthal velocity of the wave is added up to the mean flow two points are found in which the total azimuthal velocity cancels. Additionally, for a slow rotating wave, similarly to the previous case, the total azimuthal velocity of the wave can still be equal to the zonal mean velocity at some points in the domain. Therefore, figure 6c) is similar to figure 6b) except for a rotation. However, for a fast rotation of wave 2 ($\eta_1 = 0, \eta_2 = 1$) and constants $d = 2$ and $\omega_2 = -\pi/25$ on an axisymmetric flow where $\varepsilon_0 = 2.6$ and $a = 0.75$. Here also $\tau = 15$. Two filaments projecting material from the interior of the vortex are observed, and they are related to the presence

of two hyperbolic trajectories. The interior filaments recover features that are identified as interior Rossby wave breaking phenomena in de la Cámara *et al.* (2013); Guha *et al.* (2016) and are also visible from the reanalysis data as shown in Figures 1 and 4a) ($\omega_2 = 4\pi$; red line), the total azimuthal velocity of the wave will be larger than the zonal mean velocity at all points in the domain. In this case, the pattern of M (figure 6d) is very different from the pattern in figure 6b) showing no HTs.

Figures 7 e) and d) display a jet eroded in its outer part by perturbing waves with wave number 1 or 2. In e) parameters switch on a transient amplitude for Figure 7 displays the function M obtained from the kinematic model for the same mean flow of figure 6a) and different parameters for the wave 1 ($\eta_1 = 1, \eta_2 = 0$) on an axisymmetric flow in which $\epsilon_0 = -2.5$ and $a = 2$. Lagrangian structures are obtained from the function M for and 2. All the representations are for $t = 0$ and $\tau = 15$. One hyperbolic trajectory at the outer boundary of the jet is observed ejecting material of the vortex. In d) the parameters switch on a transient amplitude for a non travelling ($\omega_2 = 0$) Figure 7 a) is for the same case as figure 6b), except that the amplitude of wave 2 changes in time ($\eta_1 = 0, \eta_2 = 1$) and constant $d = 1$ on an axisymmetric flow in which $\epsilon_0 = -2.5$ and $a = 2$. Here also $\tau = 15$ and two hyperbolic trajectories. Again two HTs are visible in the external jet boundary. The filaments ejecting material in the outer part along which filamentation occurs. Figure 7 b) corresponds to just wave number 1 changing amplitude in time ($\eta_1 = 1, \eta_2 = 0$). We can see one HT at the outer boundary of the jet where material of the vortex is being ejected. In these figures, transport processes producing filamentation ejecting material, have close connections to those present in Figures 1 and 4a) that have been related, which have been linked to Rossby wave breaking phenomena at midlatitudes.

Figures 7 e) and f) show a jet which at midlatitudes Guha *et al.* (2016). In figure 7 c) the mean flow is perturbed by waves with wave numbers 1 and 2. In e) the no rotating wave 2 of figure 7 a) and wave 1 of figure 7 b) ($\eta_1 = 1, \eta_2 = 1$). In figure 7 d) the parameters are $\eta_1 = 1, \eta_2 = 1$ the same as the figure 7 c), except that wave 2 rotates ($\omega_2 = 2\pi/15$). The jet shape and filamentary structures greatly resemble those present in the reanalysis data as shown in Figures 1 and 4a).

Figures 8 present a jet which in the interior is eroded by waves 2 and 1, respectively. To achieve such a configuration, free parameters are specifically tuned including a zonal mean flow with negative velocities near the pole. In figure 8 a) the mean flow obtained with parameters $\epsilon_0 = 2.6$ and $a = 0.75$ is perturbed by just a traveling wave 2 ($\eta_1 = 0, \eta_2 = 1, d = 1, \omega_2 = -4\pi/25$) with $d = 2$. Two filaments projecting material from the interior of the vortex are observed, and they are related to the presence of interior HTs. In figure 8 b) the mean flow is obtained with the parameters $\epsilon_0 = 2.5$ and $\omega_2 = \pi/30$, representing a transient amplitude for wave one and a transient amplitude for a travelling wave two, on an axisymmetric flow in which $\epsilon_0 = -2.5$ and $a = 2$. In f) the parameters are $\eta_1 = 1, \eta_2 = 1$ with $d = 1$ and $\omega_2 = 0$, representing a transient amplitude for wave one and a transient amplitude for a non travelling wave two, on an axisymmetric flow in which $\epsilon_0 = -2.5$ and $a = 2$. The patterns are obtained for $\tau = 15$. The filamentous structures and jet shape greatly resemble those present in $a = 0.5$. This mean flow is perturbed by just a wave 1 with amplitude that varies in time ($\eta_1 = 1, \eta_2 = 0$). A protruding material filament from the interior of the vortex is observed, which is related to the presence of an interior HT. The interior filaments in these figures recover features that are identified as interior Rossby wave breaking phenomena in de la Cámara *et al.* (2013); Guha *et al.* (2016) and are also visible from the reanalysis data as shown in Figures 1 and 4a).

Figure 4b) shows the pinching of the SPV in the observations on the 24th September 2002, which is before its breakup. From the kinematic point of view the pinching is justified by the dominant presence of In the kinematic model, this structure

can be obtained with a strong Ψ_2 . However the fact that the main jet in Figure 4b) is not centered in the South pole, indicates also the presence of a component Ψ_1 . Figure ?? shows the Lagrangian patterns obtained for a non-travelling ($\omega_2 = 0$), fixed amplitude ($\eta_2 = 4, \mu = 0$) and a substantial contribution from Ψ_1 to have a displacement from the Pole. Movies S1, S2, S3 and S4 illustrate such structures. In order to reproduce the splitting we do not need to consider the displacement and thus we neglect mode 1 in what follows. Figure 9 shows a sequence of M patterns obtained with the amplitude of mean flow is given by,

$$\varepsilon_0 = \eta_0(1 + \sin(\mu t + \pi)), \quad (14)$$

where $\eta_0 = -2.5$ and $\mu = 2\pi/10$, and a stationary wave 2 with $d = 1$ overlapped with the axisymmetric mean flow obtained with $\varepsilon_0 = 1$ ($\omega_2 = 0$) with amplitude given by (13). Note that in this way the mean flow weakens as wave 2 strengthens, and $a = 0.1$, where the pinching effect is visible. The two vortices at the top and at the bottom of the pinching point would be balanced if component Ψ_1 were present. The reversal of vice-versa. The parameters fit a streamfunction which at $t = 0$ coincides with that used in figure 7a). The development of an hyperbolic point at the Pole in the axisymmetric flow described in Section 3 during the observed pinching event is in agreement with the decreasing amplitude of Ψ_0 (change of sign implies approaching to zero) and dominance of component 2. observations (figure 4b)) can be clearly seen in figure 9a). The two vortices have completely split at $t = 6$.

5 Kinematic models and conservation of Potential Vorticity

Evolution of a vorticity patch. a) Initial vorticity distribution at time t_0 ; b) Evolution of the domain with constant vorticity at time t_1 .

In this section we discuss the connection between the kinematic model introduced in the previous section and a fundamental dynamical principle of geophysical fluids. Geophysical flows that are adiabatic and frictionless conserve the potential vorticity Q along trajectories. Conservation of Q is expressed as follows:

$$\frac{dQ}{dt} = 0 \quad (15)$$

Here d/dt stands for the material derivative. A natural question here is to discuss a setting in which a whether the proposed kinematic model would conserve conserves Q .

Rossby wave breaking phenomena have been studied in simplified dynamical models by Polvani and Plumb (1992); Nakamura and Plumb (1994). These works have considered Let us assume that our setting is well approached by the quasigeostrophic motion of simple vortices in a shallow water system which is perturbed by topographically driven Rossby waves. Polvani and Plumb (1992) describe a setting (see Polvani and Plumb (1992); Nakamura and Plumb (1994)) in which Q is given by:

$$Q = f_0 + \nabla^2 \Psi - \gamma^2 \Psi + f_0 \frac{h}{D} \quad (16)$$

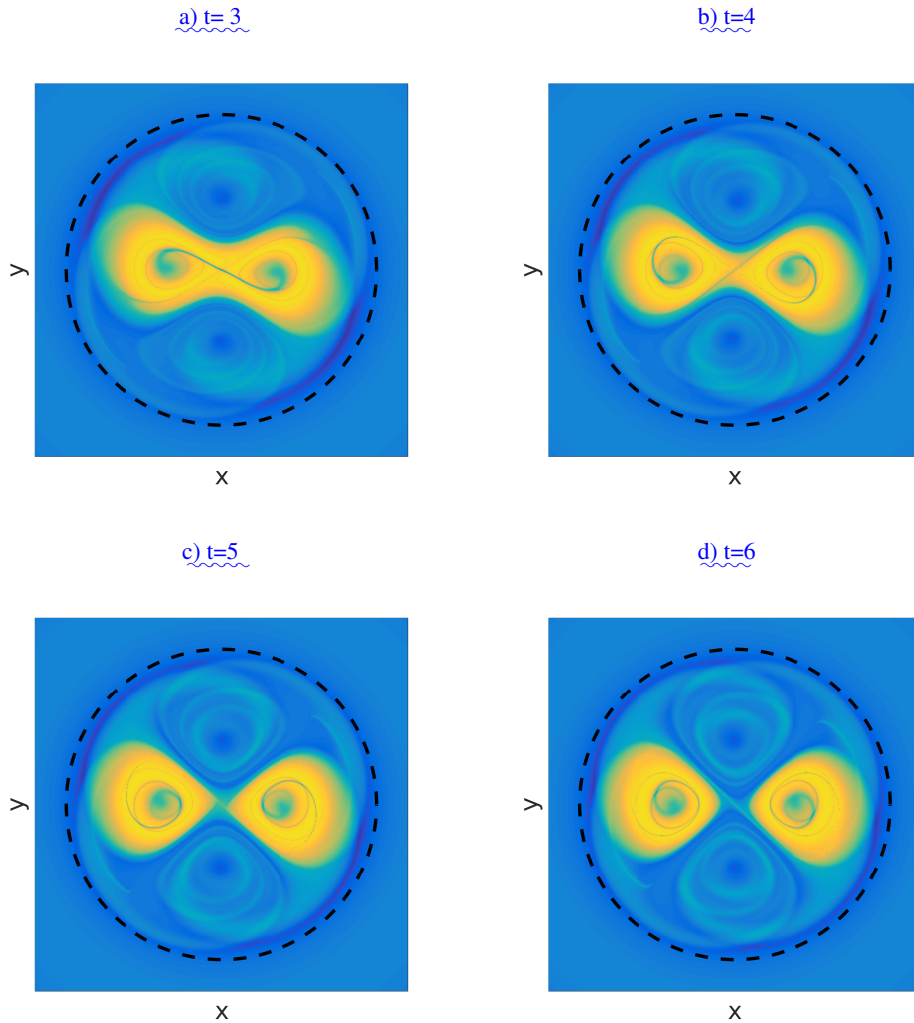


Figure 9. The function M evaluated on a stationary velocity field obtained Evolution of the Lagrangian template for a stationary non-transient wave two, $\eta_2 = 4$, $\omega_2 = 0$, $\mu = 0$ the case in which the mean flow decreases and $d = 1$ overlapped with Ψ_0 , $a = 0.1$ and $\varepsilon_0 = 1$ the wave 2 increases. The sequence reproduces many of the Lagrangian features observed in the splitting event that occurred at the end of September 2002 (see movie S5). a) $t = 3$; b) $t = 4$; c) $t = 5$; d) $t = 6$.

Here f_0 is a constant related to the rotation rate, D is the mean depth of the shallow water system, $D - h$ is the total depth, h is the bottom topography boundary of the fluid layer which is small when compared to D , and $\gamma = f_0/\sqrt{g_0 D}$, where g_0 is the gravity constant. In our setting we consider the barotropic approach with $\gamma = 0$. Ψ is the geostrophic streamfunction for the horizontal velocity field, in our case given by expression (7), with parameters corresponding to those of Figure 7 d), i.e. $\varepsilon_0 = -2.5$, $\eta_1 = 1$, $\eta_2 = 1$, $a = 2$, $d = 1$ and $\omega_2 = 2\pi/15$.

Given a vorticity distribution We assume that at the initial time, $t = 0$, the vorticity Q at an initial time, the dynamical approach computes velocities by inverting Eq. (16) for Ψ and solving the resulting equation by means of a contour dynamics algorithm (Dritschel, 1989). In the kinematic approach the field Ψ is given and we seek conditions for which Eqs. (15)-(16) hold. A first start in this discussion is to consider an initial Q distribution which consists of a constant consist of a circular patch with constant vorticity Q_0 value in the whole domain and which is kept like that for all time. In this case any fluid parcel trajectory will straightforwardly satisfy Eq. (15), as while it moves Q does not change in the domain. On the other hand, if Ψ and (constant) Q are specified, then Eq. (15) and Eq. (16) hold with appropriately chosen h .

Now we ask about other not so simple initial distributions of Q , that also satisfy Eqs. (15)-(16). The initial potential vorticity distribution discussed by Polvani and Plumb (1992) is illustrated in Figure 10 a). They consider a simple circular patch of constant value Q_0 in a domain P , surrounded by a region with also constant vorticity $Q_1 < Q_0$. This initial distribution, in our particular setting would clearly satisfy Eq. (15) for fluid parcels inside each region Q_0 and inside and vorticity Q_1 if the evolution from time t_0 to time $t_1 = t_0 + \Delta t$ keeps fluid parcels inside each region. Fluid parcels close to the boundary at t_0 would not have a problem preserving Q if the domain P at t_1 is distorted outside. At a later time $t = 2$, the vorticity distribution that preserves Eq. (15), is obtained by advecting the circular contour at $t = 0$ according to the equations of motion Eq. (12) for the prescribed Ψ , with algorithms described in Mancho *et al.* (2004). Figure 10 b) illustrates summarizes the evolution of the domain P at time t_1 and the position of fluid parcels labelled as 1,2,3 and 4 preserving vorticity. If the function Q is a time dependent function defined in this way then Eq. (15) is satisfied in our setting. We also note that Eq. (16) is satisfied if from time $t = 0$, to time $t = 2$, h is constructed from the time dependent Q function prescribed to be:

$$\frac{h}{D} = \frac{Q}{f_0} - \frac{\nabla^2 \Psi}{f_0} - 1 \quad (17)$$

Figure 11 shows the evolution of the function h/D between $t = 0$ and $t = 2$. In particular the figure shows results for $Q_0 = 2$, $Q_1 = 1.8$ and the prescribed Ψ exactly as we did in the example at the beginning of this section. Finally we $f_0 = 20$. We note that this argument can be extended to calculation could have been repeated for any initial distribution of Q defined as a piecewise constant function. Therefore the topographic forcing The lower boundary h is a thus a time dependent function adjusted to preserve the conservation of the potential vorticity. Similar settings that consider a time dependent topography (physically related to a time dependent lower layer boundary) is described by Nakamura and Plumb (1994). Without this forcing, kinematic models would not preserve potential vorticity. This latter case is discussed by Samelson and Wiggins (2006).

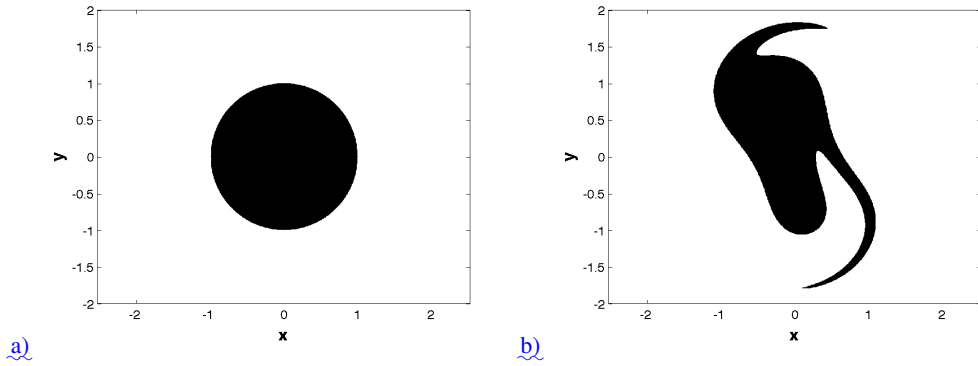


Figure 10. Evolution of a vorticity patch. a) Initial vorticity distribution at time $t = 0$; b) evolution of the vorticity at time $t = 2$.

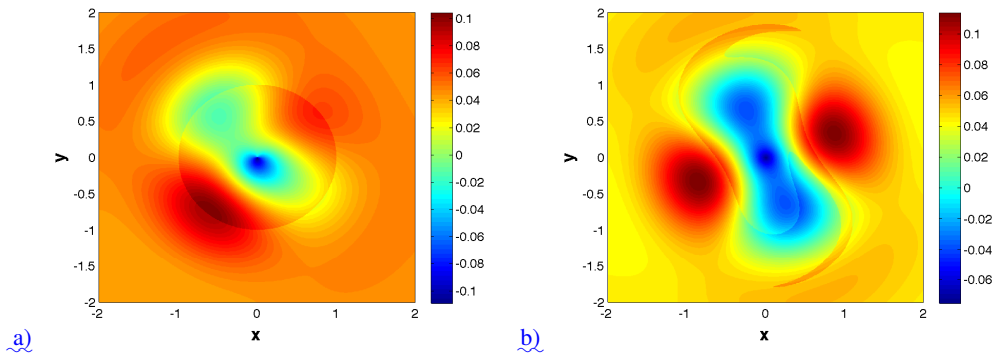


Figure 11. Evolution of the scaled lower boundary h . a) The function h/D at time $t = 0$; b) evolution of h/D at time $t = 2$.

6 Conclusions

15 In this work we propose a simple kinematic model for studying transport phenomena in the Antarctic Polar vortex. We are interested in gaining insights into the processes which carry material outwards from the ~~vortex~~-vortex structure and inwards to the vortex structure.

The construction of the kinematic model is realized by analyzing geopotential height data produced by the ECMWF. In particular our focus is on the stratospheric sudden warming event that took place in 2002, producing the pinching and then
 20 breaking of the stratospheric polar vortex. We identify the prevalent Fourier components during this period, which consist of a mean axisymmetric flow and waves with wavenumbers one and two. The kinematic model is based on analytical expressions which recover the spatial structures of these representative Fourier components. The model can be controlled so that waves with wavenumbers one and two can be switched on and off independently. We are also able to adjust the relative position of the waves with respect to the mean axisymmetric flow.

The study of Lagrangian transport phenomena in the ERA-Interim reanalysis data by means of Lagrangian Descriptors ~~highlight hyperbolic trajectories in the outer and inner part of vortex~~ highlights hyperbolic trajectories. These trajectories are ~~the Lagrangian objects that cause~~ Lagrangian objects 'seeding' the observed filamentation phenomena. The Lagrangian study of the kinematic model sheds light on the role played by waves in this regard. ~~We find that the model with just wave one, produces just one hyperbolic trajectory that can erode material either from the interior (Fig. 7 a) or exterior (Fig. 7 e) part of the jet, depending on its relative position to it. Similarly the model with just wave two, produces two hyperbolic trajectories eroding material either from the interior (Fig. 7 b) or exterior (Fig. 7 d) part of the jet, depending on its relative position. The presence of waves one and two produce~~ The model is adjusted to a stationary case which considers a mean flow and a stationary wave 2, that perturbs the mean flow in its outer part, producing hyperbolic trajectories. For the stationary case hyperbolic trajectories are easily identified. This framework is modified by transforming it to a time dependent problem by making the wave phase speed different from zero, or by introducing time dependent amplitudes. This allows to relate the time dependent structures with those easily identified in the stationary case. The setting is repeated with the wave 1, and both wave 1 and wave 2 together. The joint presence of these waves produces complex Lagrangian patterns (~~Figs. 7 e) and f)~~ remarkably similar to those observed from the analysis of the complex reanalysis data. ~~These results, and~~ confirm the findings discussed by Guha *et al.* (2016). Further adjustment of some model parameters are able to produce erosion by means of filaments just in the interior part of the flow. Finally we point out that our analysis shows that the breaking and splitting of the polar vortex is justified in our model by the sudden growth of ~~waves one and~~ wave two and the decay ~~and change of direction~~ of the axisymmetric flow.

Acknowledgements. V. J. García-Garrido, J Curbelo and A. M. Mancho are supported by MINECO grant MTM2014-56392-R. The research of C. R. Mechoso is supported by the U.S. NSF grant AGS-1245069. The research of S. Wiggins is supported by ONR grant No. N00014-01-1-0769. We also acknowledge support from ONR grant No. N00014-16-1-2492.

20 References

- Allen, D. R., Bevilacqua, R. M., Nedoluha, G. E., Randall, C. E., and Manney, G. L. (2003). Unusual stratospheric transport and mixing during the 2002 antarctic winter. *Geophysical Research Letters*, **30**(12), n/a–n/a. 1599.
- Aurell, E., Boffeta, G., Crisanti, A., Paladin, G., and Vulpiani, A. (1997). Predictability in the large: An extension of the concept of Lyapunov exponent. *J. Phys. A :Math. Gen.*, **30**, 1–26.
- 25 Bower, A. S. (1991). A simple kinematic mechanism for mixing fluid parcels across a meandering jet. *J. Phys. Oceanogr.*, **21**, 173–180.
- Bowman, K. P. (1993). Large-scale isentropic mixing properties of the Antarctic polar vortex from analyzed winds. *Journal of Geophysical Research*, **98**, 23013–23027.
- Bowman, K. P. (1996). Rossby wave phase speeds and mixing barriers in the stratosphere. part i: Observations. *Journal of the Atmospheric Sciences*, **53**(6), 905–916.
- 30 Bowman, K. P. (2006). Transport of carbon monoxide from the tropics to the extratropics. *Journal of Geophysical Research: Atmospheres*, **111**(D2).
- Charlton, A. J., O’Neill, A., Lahoz, W. A., and Berrisford, P. (2006). The splitting of the stratospheric polar vortex in the southern hemisphere, september 2002: Dynamical evolution. *J. Atmos. Sci.*, **66**, 590–602.
- Chubachi, S. (1984). Preliminary result of ozone observations at syowa station from february 1982 to january 1983. *Mem. Nat. Inst. Polar Res*, **34**, 13–19.
- 35 de la Cámara, A., Mancho, A. M., Ide, K., Serrano, E., and Mechoso, C. (2012). Routes of transport across the Antarctic polar vortex in the southern spring. *J. Atmos. Sci.*, **69**(2), 753–767.
- de la Cámara, A., Mechoso, R., Mancho, A. M., Serrano, E., and Ide, K. (2013). Isentropic transport within the Antarctic polar night vortex: Rossby wave breaking evidence and Lagrangian structures. *J. Atmos. Sci.*, **70**, 2982–3001.
- Dee, D. P. *et al.* (2011). The ERA-Interim reanalysis: configuration and performance of the data assimilation system. *Quarterly Journal of the Royal Meteorological Society*, **137**(656), 553–597.
- 5 Dritschel, D. G. (1989). Contour dynamics and contour surgery: numerical algorithms for extended, high-resolution modelling of vortex dynamics in two-dimensional, inviscid, incompressible flows. *Comput. Phys. Rep.*, **10**, 77–146.
- Esler, J. G. and Scott, R. K. (2005). Excitation of transient rossby waves on the stratospheric polar vortex and the barotropic sudden warming. *Physical Review E*, **62**, 3661–3681.
- Farazmand, M. and Haller, G. (2012). Computing Lagrangian Coherent Structures from variational LCS theory. *Chaos*, **22**, 013128.
- 10 Fueglistaler, S., Legras, B., Beljaars, A., Morcrette, J.-J., Simmons, A., Tompkins, A. M., and Uppala, S. (2009). The diabatic heat budget of the upper troposphere and lower/mid stratosphere in ECMWF reanalyses. *Quarterly Journal of the Royal Meteorological Society*, **135**(638), 21–37.
- Garcia-Garrido, V. J., Mancho, A. M., and Wiggins, S. (2015). A dynamical systems approach to the surface search for debris associated with the disappearance of flight MH370. *Nonlin. Proc. Geophys.*, **22**, 701–712.
- 15 Garcia-Garrido, V. J., Ramos, A., Mancho, A. M., Coca, J., and Wiggins, S. (2016). A dynamical systems perspective for a real-time response to a marine oil spill. *Marine Pollution Bulletin.*, pages 1–10.
- Guha, A., Mechoso, C. R., Konor, C. S., and Heikes, R. P. (2016). Modeling rossby wave breaking in the southern spring stratosphere. *J. Atmos. Sci.*, **73**(1), 393–406.
- Haller, G. (2000). Finding finite-time invariant manifolds in two-dimensional velocity fields. *Chaos*, **10**(1), 99–108.

- 20 Haller, G. (2001). Distinguished material surfaces and coherent structures in three-dimensional fluid flows. *Physica D*, **149**, 248–277.
- Haller, G. and Beron-Vera, F. J. (2012). Geodesic theory of transport barriers in two-dimensional flows. *Physica D*, **241**(7), 1680–1702.
- Haller, G. and Yuan, G. (2000). Lagrangian coherent structures and mixing in two-dimensional turbulence. *Physica D*, **147**, 352–370.
- Holton, J. R. (2004). *An Introduction to Dynamic Meteorology*. Elsevier Academic Press.
- Ide, K., Small, D., and Wiggins, S. (2002). Distinguished hyperbolic trajectories in time dependent fluid flows: analytical and computational
25 approach for velocity fields defined as data sets. *Nonlin. Proc. Geophys.*, **9**, 237–263.
- J.D.Farman, B.G.Gardiner, and J.D.Shanklin (1985). Large losses of total ozone in antarctica reveal seasonal ciox/nox interaction. *Nature*,
315, 207–210.
- Ju, N., Small, D., and Wiggins, S. (2003). Existence and computation of hyperbolic trajectories of aperiodically time-dependent vector fields
and their approximations. *Int. J. Bif. Chaos*, **13**, 1449–1457.
- 30 Juckes, M. N. and McIntyre, M. E. (1987). A high-resolution one-layer model of breaking planetary waves in the stratosphere. *Nature*, **328**,
590–596.
- Konopka, O., Groo, J.-U., Hoppel, K. W., Steinhorst, H.-M., and Muller, R. (2005). Mixing and chemical ozone loss during and after the
antarctic polar vortex major warming in september 2002. *J. Atmos. Sci.*, **62**, 848–859.
- Krüger, K., Naujokat, B., and Labitzke, K. (2005). The unusual midwinter warming in the southern hemisphere stratosphere 2002: A
35 comparison to northern hemisphere phenomena. *J. Atmos. Sci.*, **62**, 603–613.
- Lopesino, C., Balibrea-Iniesta, F., Wiggins, S., and Mancho, A. M. (2015). Lagrangian descriptors for two dimensional, area preserving
autonomous and nonautonomous maps. *Communications in Nonlinear Science and Numerical Simulations*, **27**(1-3), 40–51.
- Lopesino, C., Balibrea-Iniesta, F., García-Garrido, V. J., Wiggins, S., and Mancho, A. M. (2017). A theoretical framework for lagrangian
descriptors. to appear. *International Journal of Bifurcation and Chaos*.
- Madrid, J. A. J. and Mancho, A. M. (2009). Distinguished trajectories in time dependent vector fields. *Chaos*, **19**, 013111.
- Malhotra, N. and Wiggins, S. (1998). Geometric structures, lobe dynamics, and Lagrangian transport in flows with aperiodic time-
5 dependence, with applications to Rossby wave flow. *J. Nonlinear Science*, **8**, 401–456.
- Mancho, A. M., Small, D., Wiggins, S., and Ide, K. (2003). Computation of Stable and Unstable Manifolds of Hyperbolic Trajectories in
Two-Dimensional, Aperiodically Time-Dependent Vectors Fields. *Physica D*, **182**, 188–222.
- Mancho, A. M., Small, D., and Wiggins, S. (2004). Computation of hyperbolic trajectories and their stable and unstable manifolds for
oceanographic flows represented as data sets. *Nonlin. Proc. Geophys.*, **11**, 17–33.
- 10 Mancho, A. M., Small, D., and Wiggins, S. (2006a). A comparison of methods for interpolating chaotic flows from discrete velocity data.
Computers and Fluids, **35**, 416–428.
- Mancho, A. M., Small, D., and Wiggins, S. (2006b). A tutorial on dynamical systems concepts applied to Lagrangian transport in oceanic
flows defined as finite time data sets: Theoretical and computational issues. *Phys. Rep.*, **237**(3-4), 55–124.
- Mancho, A. M., Wiggins, S., Curbelo, J., and Mendoza, C. (2013). Lagrangian descriptors: A method for revealing phase space structures of
15 general time dependent dynamical systems. *Communications in Nonlinear Science and Numerical Simulations*, **18**(12), 3530–3557.
- Manney, G. L. and Lawrence, Z. D. (2016). The major stratospheric final warming in 2016: Dispersal of vortex air and termination of Arctic
chemical ozone loss. *Atmospheric Chemistry and Physics Discussions*, **2016**, 1–40.
- Manney, G. L., Farrara, J. D., and Mechoso, C. R. (1991). The behavior of wave 2 in the southern hemisphere stratosphere during late winter
and early spring. *J. Atmos. Sci.*, **48**, 976–998.

- 20 Manney, G. L., Sabutis, J. L., Alley, D. R., Lahoz, W. A., Scaife, A. A., Randall, C. E., Pawson, S., Naujokat, B., and Swinbank, R. (2006). Simulations of dynamics and transport during the september 2002 antarctic major warming. *J. Atmos. Sci.*, **66**(690-707).
- McIntyre, M. E. and Palmer, T. N. (1983). Breaking planetary waves in the stratosphere. *Nature*, **305**, 593–600.
- McIntyre, M. E. and Palmer, T. N. (1984). The surf zone in the stratosphere. *Journal of Atmospheric and Terrestrial Physics*, **46**(9), 825–849.
- McIntyre, M. E. and Palmer, T. N. (1985). A note on the general concept of wave breaking for rossby and gravity waves. *Pure and Applied Geophysics*, **123**(6), 964–975.
- 25 Mechoso, C. R., O’Neill, A., Pope, V. D., and Farrara, J. D. (1988). A study of the stratospheric final warming of 1982 in the southern hemisphere. *Quarterly Journal of the Royal Meteorological Society*, **114**(484), 1365–1384.
- Mendoza, C. and Mancho, A. M. (2010). The hidden geometry of ocean flows. *Phys. Rev. Lett.*, **105**(3), 038501.
- Mendoza, C. and Mancho, A. M. (2012). The Lagrangian description of aperiodic flows: a case study of the Kuroshio Current. *Nonlin. Proc. Geophys.*, **19**(14), 449–472.
- 30 Mendoza, C., Mancho, A. M., and Wiggins, S. (2014). Lagrangian descriptors and the assesment of the predictive capacity of oceanic data sets. *Nonlin. Proc. Geophys.*, **21**, 677–689.
- Morales-Juberías, R., Sayanagi, K. M., Simon, A. A., Fletcher, L. N., and Cosentino, R. G. (2015). Meandering shallow atmospheric jet as a model of saturn’s north-polar hexagon. *The Astrophysical Journal Letters*, **806**, L18 (6pp).
- 35 Nakamura, M. and Plumb, R. A. (1994). The effects of flow asymmetry on the direction of rossby wave breaking. *J. Atmos. Sci.*, **51**, 2031–2044.
- Ottino, J. M. (1989). *The Kinematics of Mixing: Stretching, Chaos, and Transport*. Cambridge University Press, Cambridge, England. Reprinted 2004.
- Plumb, R. A. (2007). Tracer interrelationships in the stratosphere. *Reviews of Geophysics*, **45**(4).
- Polvani, L. M. and Plumb, R. A. (1992). Rossby wave breaking, microbreaking, filamentation, and secondary vortex formation: The dynamics of a perturbed vortex. *J. Atmos. Sci.*, **49**(6), 462–476.
- Quintanar, A. I. and Mechoso, C. R. (1995). Quasi-stationary waves in the southern hemisphere. part i: Observational data. *J. Climate*, **8**, 2659–2672.
- 5 Rabier, F. *et al.* (2010). The concordiasi project in antarctica. *Bulletin of the American Meteorological Society*, **91**(1), 69–86.
- Rypina, I. I., Brown, M. G., Beron-Vera, F. J., Kocak, H., Olascoaga, M. J., and Udovychenkov, I. A. (2007). On the lagrangian dynamics of atmospheric zonal jets and the permeability of the stratospheric polar vortex. *J. Atmos. Sci.*, **64**, 3595–3610.
- Samelson, R. and Wiggins, S. (2006). *Lagrangian Transport in Geophysical Jets and Waves: The Dynamical Systems Approach*. Springer-Verlag, New York.
- 10 Samelson, R. M. (1992). Fluid exchange across a meandering jet. *J. Phys. Oceanogr.*, **22**(4), 431–440.
- 570 Shadden, S. C., Lekien, F., and Marsden, J. E. (2005). Definition and properties of Lagrangian Coherent Structures from finite-time Lyapunov exponents in two-dimensional aperiodic flows. *Physica D*, **212**, 271–304.
- Simmons, A., Uppala, S., Dee, D., and S, K. (2007). ERA-Interim: New ECMWF reanalysis products from 1989 onwards. *ECMWF Newsletter*, **110**, 25–35.
- Smith, M. L. and McDonald, A. J. (2014). A quantitative measure of polar vortex strength using the function m. *J. Gephys.Res. Atmos.*, **119**, 5966–5985.
- 575 Snyder, J. P. (1987). *Map Projections—A Working Manual*. U.S. Geological Survey professional paper. U.S. Government Printing Office.
- Solomon, S. (1988). The mystery of the antarctic ozone “hole”. *Review of Geophysics*, **26**, 131–148.

- Solomon, S. (1999). Stratospheric ozone depletion: review of concepts and history. *Review of Geophysics*, **37**, 375–316.
- Stewartson, K. (1977). The evolution of the critical layer of a rossby wave. *Geophysical & Astrophysical Fluid Dynamics*, **9**(1), 185–200.
- 580 Taguchi, M. (2014). Predictability of major stratospheric sudden warmings of the vortex split type: Case study of the 2002 southern event and the 2009 and 1989 northern events. *J. Atmos. Sci.*, **71**, 2886–2904.
- Varotsos, C. (2002). The southern hemisphere ozone hole split in 2002. *Environmental science and pollution research international*, **9**(6), 375–6. Copyright - Ecomed Publishers 2002; Última actualización - 2014-08-30.
- Varotsos, C. (2003). What is the lesson from the unprecedented event over antarctica in 2002. *Environmental science and pollution research international*, **10**(2), 80–1.
- 585 Varotsos, C. (2004). The extraordinary events of the major, sudden stratospheric warming, the diminutive antarctic ozone hole, and its split in 2002. *Environmental science and pollution research international*, **11**(6), 405–11.
- Warn, T. and Warn, H. (1978). The evolution of a nonlinear critical level. *Studies in Applied Mathematics*, **59**(1), 37–71.